Chapter 24

Mechanical Strength and Reliability of Glass Fibers

Charles R. Kurkjian and M. John Matthewson

Photonic Components Reliability Group, Department of Materials Science and Engineering, Rutgers University, Piscataway, New Jersey

24.1 INTRODUCTION

Silica-based light-guide fibers have been produced and deployed with great success in spite of their well-known "brittleness." For instance, techniques have been developed that allow long lengths (tens of kilometers) of such fibers to be drawn and coated in-line. The preform and draw processes allow production fiber that has a flaw-free surface with, essentially, the theoretical strength under the conditions of use/test (~5.5 GPa) for most of its length. The few manufacturing defects that occur are eliminated by a proof-testing procedure that allows the remaining length of fiber to attain almost any desired guaranteed strength. While the commonly specified proof stress is approximately 700 MPa, by reducing the available continuous lengths and at some increase in cost, higher proof stresses are possible. Success of this sort has not been achieved with all glass fibers, however. Multicomponent silicate fibers, hollow waveguides, and photonic crystal guides have been studied much less, and while their capabilities can be predicted to some extent, very few data are available. The mechanical properties of other specialty glass fibers, such as heavy-metal fluoride (HMF), telluride, and chalcogenide glasses, have also been studied with varying degrees of success.

Intensive study and modification of the processes used for manufacturing the fiber preforms and the resulting fiber have resulted in the very high quality fiber described earlier. The use of very high quality raw materials for the core and cladding, control of the purity of the gases employed in the furnace, as well as control of the solid and gaseous impurities available to interact with the hot fiber in the draw environment proved very important in this regard. Because it was known that contact of the pristine fiber surface with any hard material would

easily cause surface damage and a precipitous reduction in strength, techniques were developed very early to enable a protective polymer coating to be applied in-line without itself causing damage to the fiber surface. Because of the purity of all of the materials employed, there are rarely any solid impurity particles in the body of the fiber, so in almost all cases, the strength of the fiber is the strength of its surface. Thus, the condition of the surface of the fiber determines its strength. Whatever the situation with regard to the "starting" strength of any given fiber or fiber type, several things must be kept in mind:

a. Fibers are normally coated in-line with a polymer, which provides protection from mechanical damage. The strength of bare fiber can be easily reduced precipitously by the development of such mechanical damage on the glass surface. The damage is the result of the contact of hard foreign particles on the glass surface, which produce strength reducing cracks or scratches. Such strengths show a very broad distribution and are unpredictable.
b. Delayed failure or fatigue causes the initial strength to decrease with time under load in glasses of most compositions.
c. In some cases, strength decreases are noted with time under "severe" conditions, even in the absence of an applied stress; this is termed "zero stress aging."
d. Glasses are essentially "frozen" liquids with no regular lattice, but with a random structure and fluctuations characteristic of a liquid. They are in a metastable state with respect to the crystal and heating to a critical temperature where crystallization may occur at a reasonable rate will certainly lead to strength degradation. Even if there is no crystallization, there may be relaxation of the glass structure and, therefore, changes in the glass properties that must be kept in mind when processing fibers for use in some applications.

24.2 REVIEW OF GLASS PROPERTIES

In this section, we review some of the important parameters of glass systems that can affect their mechanical behavior and mechanical reliability.

24.2.1 Noncrystallinity, the Glass Transition (T_g), and Relaxation Processes

Although there are several operational definitions of "glass," for our purpose, we define a glass as a material that has been cooled from the melt without crystallizing. In the region from T_m, the melting point and T_g, the glass transition temperature (the temperature at which the viscosity, $\eta \sim 10^{12.4}$ Pa/sec), the

material is called a "supercooled" liquid (Fig. 24.1, [1]). In this state, it has the structure of the liquid, and although the mobility of the structure is reduced as the temperature is reduced, structural rearrangements can occur in experimental times. Because of this, the coefficient of thermal expansion is substantially higher (~2–3 times) than below T_g.

As seen in Fig. 24.1, changes in cooling rate from T_g will result in changes in room temperature properties such as density and refractive index. To a very rough approximation, we may consider these materials to behave as maxwellian solids, with $\eta = G\tau$, where G is the shear modulus and τ the shear relaxation time; at T_g, relaxation times of the order of minutes are found. Thus, metastable equilibrium is achieved in reasonable experimental times. Below T_g, relaxation increases with an activation energy of the order of 400–1000 kJ/mol, and thus, major structural changes cannot usually occur in experimental times. However, in the case of rather rapidly quenched materials, such as silica fibers, it has been found that substantial relaxations can occur below T_g.

Below T_g the mobility is so small that structural rearrangements do not occur in experimental times. This material is considered to be in the amorphous

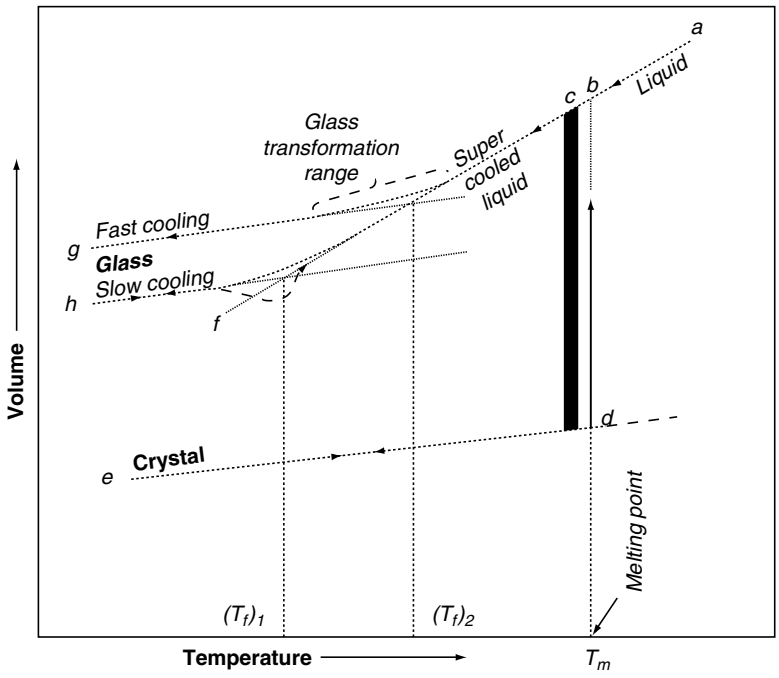

Figure 24.1 Schematic of the glass transition (used, with permission, from reference [1]).

or glassy state. On cooling from T_g to room temperature, the linear thermal expansion is the result of changes in bond lengths, whereas above T_g, a thermal expansion coefficient, which is at least twice as great, is due to structural rearrangements and to bond length changes. For materials such as silica, silicates, and some chalcogenides, upon reheating through T_g and up to the melting point, there is little probability of crystallization when heating at reasonable rates. Other glasses such as the HMFs may rather easily crystallize on either reheating or on the initial cooling. Thus, in such glasses, care must be taken to ensure that no crystallization occurs. In particular, surface-nucleated crystallization may be a problem both mechanically and optically.

Glasses differ from their crystalline counterparts in that their structure has no repeating lattice but is instead random. There may be both chemical and structural randomness, which may give rise to optical scattering. Regions of chemical or structural fluctuations may lead to fluctuations in solution rate as well. We postulate that this may lead to the zero stress aging described later.

24.2.2 Brittleness, Hardness, and Cracking

Most of the inorganic glasses with which we are concerned fail in a brittle manner. That is, they will fail by fast fracture (i.e., cracks that grow unstably to produce rapid and complete failure without any significant ductile deformation). Brittle materials are sensitive to the presence of cracks and other stress-concentrating defects, and if mishandled, it is possible to introduce significant damage with corresponding weakening. As a result, glasses are frequently mistakenly described as ''brittle'' if they are weak and easily break on handling. However, this is incorrect because ''brittle'' refers to crack propagation without ductility; whereas brittle materials are often weak, they can also be extremely strong if severe strength-degrading defects are avoided or eliminated. Pure silica and silicate glasses have high intrinsic strengths that are higher than most ''strong'' ductile metals. However, their brittleness means they are easily damaged. Contact of the newly drawn perfect surface of a silica light-guide fiber with a sharp hard object will result in an instantaneous and serious reduction in strength, by a factor up to 100 or more. The susceptibility to surface damage (cracking) is not easily understood or predicted. Although, as just stated, the glasses with which we are concerned are basically brittle, under the action of a complex state of applied stress such as found under a sharp indenter or scribe, they will flow at room temperature. This flow will result in the development of residual stresses and ultimately lead to the generation of cracks. Also, even blunt indenters, if subject to a high enough load, will result in the generation of cracks. Two investigations in the literature illustrate this nicely. Baikova et al. [2] studied the behavior of a glass plate when indented with a 2-mm diameter steel ball.

Their initial results showed a great deal of scatter in the load required to produce cracking and thus considerable variability in the strength reduction, certainly at loads in the range of 20–100 N, and occasionally at substantially lower loads. After cleaning the ball and the glass surface, they found the higher loads were required to cause fracture, and from this, they deduced that the presence of dust particles was the cause of the very much lower loads. With a clean ball on a clean surface, the load necessary to cause cracking and thus lower the strength of a silica plate was found to be approximately 100 N, in agreement with that predicted for this situation in which a ball is loaded on a flat substrate. In this case, the tensile stress that induces cracking is just outside the contact area, roughly the diameter of the ball. One of the present authors [3] has shown more quantitatively that the use of an indenter in the shape of the corner of a cube, rather than the much more blunt Vickers pyramid indenter with a 138-degree included angle, results in a reduction of the load to cause cracking by two orders of magnitude (<2 mN versus 2 N or more) (Fig. 24.2). In the case of the cube corner indenter, cracking is produced during loading and the appropriate equation to describe this effect is

$$P_r \sim P\left(\frac{E}{H}\right)^{1/2} \cot \psi^{2/3}, \tag{24.1}$$

where P_r is the crack opening force due to the applied load P, E is Young's modulus, H the hardness, and ψ is the indenter angle [4]. In the case of the

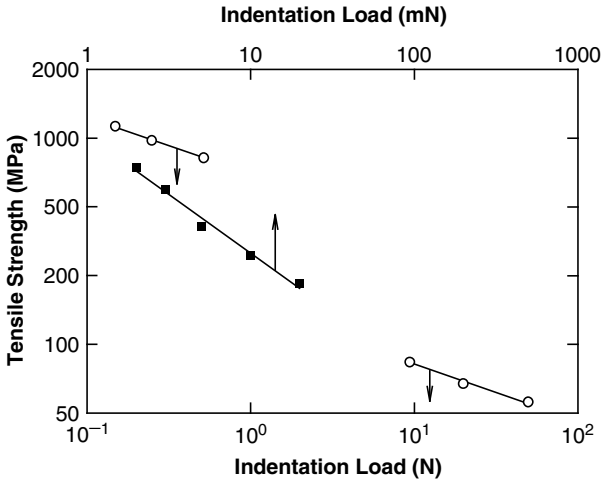

Figure 24.2 Comparison of the effect of indentation load on the resultant strength of silica fibers: Vickers (circles, bottom scale) and cube corner (squares, top scale) (data used, with permission, from reference [3]).

blunter Vickers pyramid indenter, cracking may occur on unloading and, therefore, is driven by the residual stresses developed during the plastic deformation associated with formation of the permanent impression.

24.2.3 Composition Effects

Table 24.1 lists a number of typical inorganic glasses that may be of use as light guides or in light-guide devices, together with some of their important properties. E is the Young's modulus, K_{IC} is the fracture toughness, H_V is the Vickers hardness, T_g is the glass transition temperature, and α is the coefficient of thermal expansion. Columns five through eight list some strength values and are described later. As indicated earlier, glasses are often referred to as *brittle,* whereas as can be seen here, they can have exceptionally high intrinsic strengths.

24.2.3.1 Silicates

The vast majority of commercial glasses are so-called multicomponent glasses (MCGs) that contain three to six oxide components. Early in the development of light-guide fibers, many workers attempted to employ these well-known and well-characterized glasses for long-length communications [5–7]. It was found very difficult to purify them to the extent necessary for low optical loss. In addition, it was found quite early on that by using vapor-phase processes and extreme purity liquid precursors for the preparation of pure glass-former glass fibers, high purity could be maintained throughout the fiber production. However, even so, it was not possible to produce MCG fibers because suitable liquid precursors were generally not available. In addition, simple two-component alkali silicates that were predicted to have ultimate scattering losses lower than silica could not be used because at the low alkali concentrations desired, phase separation was encountered [8]. Also, the addition of even small amounts of these oxides results in a glass with very different viscosity and thermal expansion, so processing of these with a silica cladding becomes difficult. Duncan et al. [9] looked at alkali and alkaline earth borosilicate glasses (silica and NBS glass), but as indicated earlier, had problems with purity. Figure 24.3 is a Weibull probability plot (see the later section on Weibull statistics) of the distributions of the strength of silica and an NBS glass and it is seen that reasonable strengths were obtained for such glasses, but their purity, and thus, optical transmission, was poor. In the future, it may be desirable to employ such glasses, if extremely low losses are not required, because their mechanical properties may be suitable.

In Fig. 24.3, we present failure strain rather than failure stress/strength. The reason for this is that a common technique used for testing these fibers

Table 24.1

Mechanical properties of various glasses

Glass	E GPa	K_{IC} MPa/m$^{1/2}$	H_V GPa	σ^a GPa	$E/5$ GPa	σ_K GPa	% theoretical[c]	n	T_g °C	$\alpha 10^{-6}/°C^{-1}$
Silica	72	0.75	14	14 (77 K)	14	14	100 (14/14)	20	1150	5
SLS	70	0.75	5.5	7.7 (77 K)	14	14	40 (5.5/14)	15	550	85
Chalcogenide	10–20	0.15–0.25	1.0–1.9	1.2 (300 K)	2–4	4.7	50–100 [2.4/(2–4)]	10–20	200–300	100–600
HMF	50–65	0.2–0.5	2.5–3.0	1.0–1.6 (300 K)	10–13	9.3	35 (3.2/9.3)	0–60	250–400	150–200
Tellurite	45	0.25–0.3	3.0–3.8	0.82 (300 K)	9	5.6	30 (1.6/5.6)	?	350	150

[a] Highest measured strengths at temperature given in parenthesis.
[b] Strengths are calculated using K_{glass}/K_{silica} from Eq. 24.3, assuming the initial sizes are equal.
[c] Strengths at 77 K are divided by the lower value from columns 5 or 7. The room temperature strengths in column 5 have been multiplied by 2 to approximate strengths at 77 K.

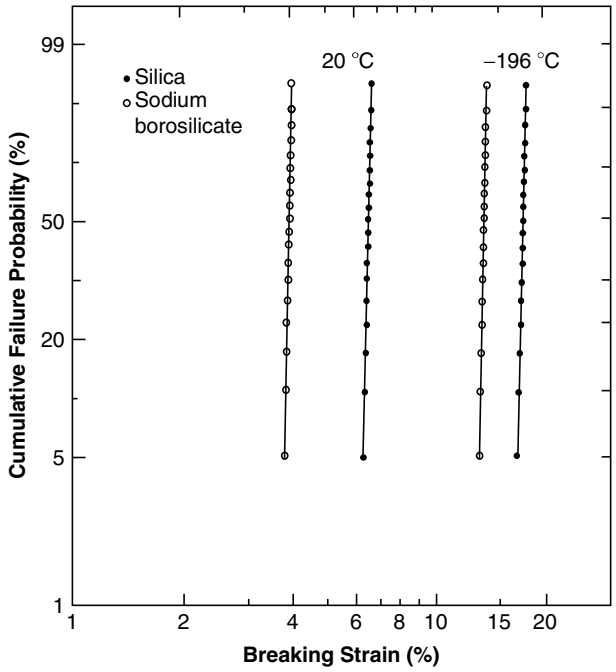

Figure 24.3 Failure strain (measured in two-point bend) of silica (●) and sodium borosilicate (○) glass fibers in liquid nitrogen and at room temperature (used, with permission, from reference [9]).

has been two-point bending rather than the more usual tension testing. Bending measurements directly determine the strain to failure and the elastic modulus is needed to convert to failure stress. Because the modulus is often not known, it is simpler to report failure strain, as has been discussed in the literature [10]. In a later section, the conversion of strain to stress is described in more detail.

24.2.3.2 Tellurite Glasses

Although tellurium dioxide does not form a glass in its pure state, oxide glasses based on TeO_2 have been found to have desirable light-emitting properties when doped with rare earth ions. In particular, the optical behavior of these glasses has been studied extensively for use as erbium-doped fiber amplifiers. To our knowledge, only one study of the mechanical strength of these glasses has been carried out [11].

24.2.3.3 Nonoxide Glasses

Because of their atomic sizes, bond types and bond strengths, oxide glasses show very strong optical absorptions in the near infrared (IR). Although the near-IR band edge may be moved somewhat further into the IR by using large heavy atoms in a silicate glass or by going to a germanium-based glass, to shift the band edge substantially, glasses based on anions other than oxygen are required. For this purpose, chalcogenide and HMF, non-silicate, nonoxide glasses have been studied intensively.

24.2.3.3.1 Chalcogenides

Although chalcogenide glasses were studied as early as 1912 [12], serious study of the individual chalcogens and chalcogenide glasses was not undertaken until the 1960s when interesting electronic properties were discovered [13, 14].

Chalcogenide glasses can be formed over a very wide range of composition. They contain one or more of the elements sulfur, selenium, or tellurium (chalcogens) with other elements from groups IV, V, and VI of the periodic table. For glasses having good transmission in the near IR (0.5–10 μm), most attention is now paid to glasses in the general composition ranges of As-S, As-Se, Ge-As-S, and Ge-Se-Te. Extrinsic absorption is most often caused by the presence of impurities of oxygen and hydrogen.

24.2.3.3.2 Heavy-Metal Fluorides

In 1975, Poulain et al. [15] unexpectedly discovered a fairly large range of glass-forming compositions based on HMFs; specifically zirconium fluoride. There followed a period of intense study because it had been shown theoretically that for highly pure glasses in these systems, there was the possibility of ultimate optical losses substantially lower than those for silica. It has subsequently been found impossible to produce either bulk glass or fibers with impurity levels sufficiently low for these theoretical losses to be realized. In addition, the difficulties with crystallization during fiber drawing restrict the compositions that are practically useful. However, they are still of some interest for certain applications.

Compositions most studied are ZBLAN (fluorides of zirconium, barium, lanthanum, and sodium) and ZBLAN with additions of AlF_3 [16].

24.2.3.4 Photonic Crystal Fibers

Photonic crystal fibers or ''holey'' fibers are just that. They are fibers having holes distributed over their cross-section [16]. Because they are normally a single

material and normally silica, their material properties are the same as the materials listed in Table 24.1.

24.3 MECHANICAL PROPERTIES

In most of this section, we deal with general glass properties or with those of silica fibers. In the final portions of the section, we review nonsilica fiber properties.

In Table 24.1, columns five through eight, some data on the strengths of a variety of glasses are given. In column 5, the highest reported measured strengths are given, with the measurement temperature indicated in parenthesis. For silica and the soda-lime–silica glass, these are strengths measured at 77 K for what are thought to be flaw-free samples. The value for silica is the same as that for a silica-clad light-guide fiber because in this case the strength-controlling surface is composed of silica. We designate these *intrinsic inert strengths*—strengths measured on samples with no flaws under conditions where no delayed failure or fatigue can occur (77 K). Columns 6 and 7 give two approximations for the theoretical strengths. The first (column 6) is an approximation based on the fact that the strength is expected to be a substantial fraction of the elastic (Young's) modulus, in this case, we list $E/5$. It is seen that this gives the value measured for silica. Column 7 is an estimate based on the proportionality of strength (σ) and fracture toughness (K_{IC}) for a given flaw size, c, in Eq. (24.3). Here, it is assumed that the effective "crack" size in all glasses is the same and the data are normalized to the value of 14 GPa for silica. Column 8 is the ratio of the highest measured strength (estimated at 77 K as twice the room temperature value) to the lowest estimated theoretical value. As indicated, the value for silica is the theoretical value. For all other glasses except for As_2S_3, the percentage is 30–40%. For As_2S_3, it is possible that the fibers for which the measured strength at room temperature is 1.2 GPa may be very close to the inert, intrinsic, or theoretical "flaw-free" strength, approximately 2.4 GPa at 77 K.

24.3.1 Strength

24.3.1.1 Inert, Intrinsic Strength: Tension and Two-Point Bend

Figures 24.4 and 24.5—from the very important work of Proctor, Whitney, and Johnson in 1967 [17]—illustrate a number of significant points that we discuss later in this section. This work was carried out at Rolls Royce because of its interest in developing stronger aluminum aircraft parts by using silica fiber reinforcement. Figures 24.4 and 24.5 show the very significant temperature and

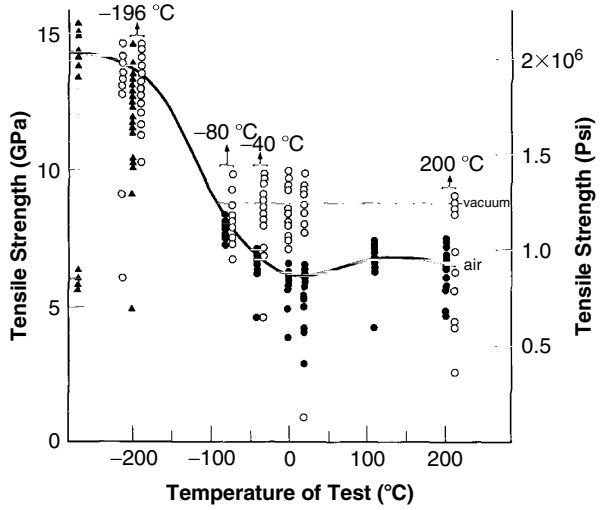

Figure 24.4 Effect of temperature on the tensile strength of silica fibers. Fibers were tested in the following environments: × liquid helium or nitrogen, ○ *in vacuo*, ● air, ▲ gaseous hydrogen (used, with permission, from reference [17]).

time dependence of the tensile strength of silica fibers. These figures are of great significance and are critical to the understanding of silica and silicate fiber strength. They essentially show the effect of water vapor on the "instantaneous" strength of a silica fiber. Two things should be noticed. The large increase in strength as the temperature is lowered below room temperature, and the time dependence of the strength at room temperature are both manifestations of

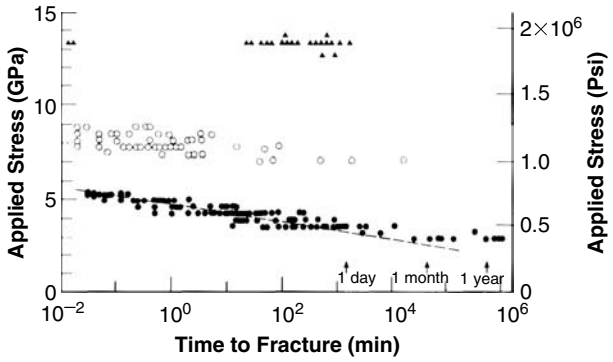

Figure 24.5 Effect of time on the tensile strength of silica fibers. × 77K, ○ *in vacuo*, ● ambient (used, with permission, from reference [17]).

"fatigue" or delayed failure. This is discussed in detail later. Here, we simply state that by testing under conditions in which the effects of moisture are eliminated (e.g., in a vacuum or at low temperature), there is no time dependence of strength; this is then termed the "inert" strength. Figure 24.3, from Duncan et al. [9] shows the inert failure strain measured at 77 K in two-point bending for fibers of silica and a sodium borosilicate glass (mentioned earlier). These latter data are shown to illustrate two important points. First, these data are plotted on a Weibull probability scale [18], as described later. The high value of the slope of the lines indicates that the strength distribution is very narrow. Second, many investigations of light-guide glass compositions, silicates, and the other glass types we discuss have employed the two-point bending technique for the study of the strength of these fibers. This technique has been described by a number of workers and has often been used in the study of light-guide fibers because of its ease and adaptability to many temperatures and environments [19]. However, this measurement method gives failure strain rather than failure stress/strength. It is known that the Young modulus (E) of silica and other silicate glasses are rather substantial functions of strain [20]. While little is known about the details of this nonlinear behavior, it is known that silica is anomalous in this regard. Its Young modulus increases with strain to at least approximately 10% strain, whereupon it decreases in a more normal way. In the evaluation of strength from failure strain at room temperature where the strain is less than 5–6%, the following equation is valid [21]:

$$\sigma = E\varepsilon;\ E = E_0(1 + \alpha\varepsilon), \tag{24.2}$$

where E_0 is the Young modulus in the limit of zero strain (72 GPa) and α corrects for the strain dependence of modulus. The accepted value of α for fused silica is 3 [21] for simple tensile stresses. However, asymmetry in the elastic modulus for tensile and compressive strains leads to a shift in the neutral axis of bent fiber such that the effective value of α that should be used for converting between bending stress and bending strain is 2.125 [22]. Thus, at room temperature where the initial failure strain in air is about 7%, the corresponding E is 83 GPa or about 15% higher for bending. While E at greater strains is not known exactly, it appears that at about 20% strain, the value at 77 K, the modulus has essentially returned to its zero-strain value of 70 GPa or so. This can be seen by dividing the 12.5 GPa strength measured by Proctor et al. [17] by the failure strain of 18% measured by France et al. [23] to give $E_{\varepsilon=18\%}$ approximately 69.4 GPa. Another example is that of a standard window or bottle glass composition, so-called soda-lime–silica glass. Ernsberger [24] has found a strength of approximately 7.7 GPa at 77 K, while Lower [25] has found a failure strain of approximately 17.7%. Thus, $E_{\varepsilon=17.7\%} \sim 43.5$ GPa whereas $E_0 \sim 72$ GPa. Very little is known about the strain dependence of E for other common silicate glasses.

In the preceding examples, we have shown data for strengths when there is no fatigue. In these cases, we have also chosen data for glasses that by our criterion [26] are flaw free. Thus, these strengths are inert, because they are free from atmospheric corrosion effects. Also, because they are flaw free, these strengths are considered intrinsic, that is, they are representative of the material and are not affected by the presence of flaws. A paper by one of the present authors has been concerned with a description and definition of intrinsic inert strength. It is suggested that the following criteria are necessary for intrinsic strength: The strength should be high with an essentially infinite Weibull modulus (i.e., the strength is single-valued), and therefore, there will be no size dependence of this strength (either fiber length or diameter). Results from Duncan et al. [9] show the room temperature and 77 K failure strains for silica, as well as for a borosilicate glass that had early been the subject of much study as a glass for possible light-guide use (Fig. 24.3). As can be seen, these failure strains are high and basically single valued. In addition, these measurements were made at 77 K. This has the effect of eliminating the effect of water in the ambient, so there is no delayed failure/fatigue. These measurements are thus "inert."

24.3.1.1.1 Flaws

As mentioned earlier, if there are no flaws, the strength is intrinsic. In practice there will be flaws of varying types, sizes, severity, distribution in length, and so on, as discussed later in the section on Weibull analysis. Flaws may be the result of scratching, adherence of solid foreign particles, or a change in the geometry of the fiber surface (see later discussion on aging). Reduction in strength may not be the result of a stress enhancement per se, but simply the result of a residual stress, perhaps because of a change in composition of the glass because of an impurity or an indentation too small to produce a crack. In the case of a residual compressive stress, it will simply be added to the applied stress in calculating failure stress.

In most cases, flaws produced as described earlier will initially have a sharp tip and the strength reduction resulting from this is one of the following:

Sharp flaws:

$$\sigma = \frac{K_{IC}}{Yc^{1/2}}, \tag{24.3}$$

where σ is the strength, K_{IC} is the critical stress intensity factor or toughness, and Y is the crack shape parameter (normally taken to be $\sim$1.24), and c is the crack length.

Blunt flaws:

In the preceding discussion, we have been concerned with cracks that have sharp tips and can thus be described by Eq. (24.3). In a later section, we deal

with flaws that have a rounded tip. In this case, assuming an elliptically shaped flaw:

$$\sigma_a = \frac{\sigma_u}{1 + 2(c/b)}, \tag{24.4}$$

where σ_u is the ultimate strength (i.e., the intrinsic strength of the material), σ_a is the applied stress, and the denominator represents the stress concentration factor at the "crack" tip, where c is the major and b the minor axis of the elliptical flaw. Such macroscopically blunt flaws were studied by Inniss et al. [27] and are described in a later section on aging.

24.3.1.2 Effect of Fiber Diameter

In spite of experimental studies showing no such effect, there is often still the perception that the strength of glass fibers increases as the diameter decreases in fiber diameter. This is primarily due to the classic paper of A. A. Griffith in 1920 [28]. In this work, he showed that the strength of a common soda-lime silicate glass (SLS) was a strong function of the fiber diameter. While this idea persisted for some time and is often still believed today, this effect was shown to be false by Otto in 1955 [29] for a similar glass, E-glass, and perhaps more completely and convincingly by Cameron in 1960 [30]. For these MCGs, it would appear that fibers must be drawn above T_l, its liquidus temperature (the temperature at which the last crystal melts), in order for a high strength single-mode distribution to be obtained. When drawn at lower temperatures, which would normally be the case when drawing thicker fibers, a lower strength mode appears. Thus, the mean or average strength of this fiber diameter will be lower than is expected for that diameter. Cameron showed clearly that the high strength mode was independent of diameter for these E-glass fibers.

While this diameter independence has not been demonstrated unequivocally in silica, the outstanding evidence is such as to be convincing. First, the essential constancy of the strength results on silica over the years, apparently independent of drawing conditions, show closely similar results. The work of Proctor et al. [17] shown in Figs. 24.4 and 24.5 was carried out on fibers of 20- to 80-μm diameter and they indicate no effect of diameter on strength. Most high-quality studies of the strength of silica for light guides have been made on 125-μm diameter fibers and have shown essentially the value found by Kurkjian and Paek [31], namely approximately 5.5 GPa at room temperature, which is very similar to the value found by Proctor et al. at room temperature [17]. There have been few other studies of the tensile strength of silica glass at 77 K. However, Smith and Michalske [32] measured 35-μm silica fibers in tension at UHV ($<6.6 \times 10^{-6}$Pa) at room temperature and found strengths approximately 11–14 GPa. Because it may be assumed that measurements at this high vacuum

condition would be essentially inert, as were those of Proctor et al. at 77 °K, this agreement is expected. It is also interesting to note that Griffith himself showed that the strengths of silica rods of 2-mm diameter were about 7 GPa at room temperature. While this was a crude bending measurement, it was firm enough and to Griffith, essentially unexplainable, so that he exempted it from his consideration of the diameter effect.

The interest in nano materials has just produced some interesting results in this regard. The group of Mazur [33] at Harvard has been studying the optical guiding behavior of silica fibers of diameters less than the wavelength of light (see Chapter 11 for more details). They have made initial efforts to measure the strength of these fibers in both tension and two-point bending. While the diameter control is very good (better than 0.1%) due to the clever "self-modulating" technique used to draw these "nanowires," both of these testing techniques are difficult with fibers of this size, so the scatter in the data is quite large (Weibull modulus ~5). While their data seem to show a dependence of strength on diameter, within the statistics, there is no significant dependence and the mean value of the combined results of tension and bending is approximately 5 GPa, not too different for that normally found for 125-μm light-guide fibers. Additional work on these fibers would appear to be warranted. All of these data are in Fig. 24.6, together with results for optical fiber with diameters up to 1 mm [34]. We will consider there to be no effect of fiber diameter on strength.

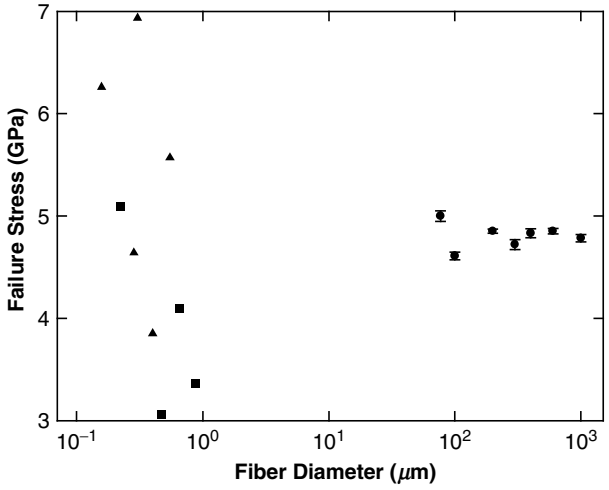

Figure 24.6 Effect of diameter on the strength of silica fibers measured in ambient on the time scale of approximately 10 seconds. Measurements: ● two-point bending, averaged for several measurements [34], ▲ two-point bending single measurements [33], ■ tension single measurements [33].

24.3.1.3 Effect of Ambient Chemistry

Later in this chapter, we discuss in detail the effects of ambient chemistry on the time dependence of strength. Here we simply show how changes in two important environmental parameters affect the short time strength (i.e., the strength recorded in seconds at room temperature). Figure 24.7 [35] shows the effect of ambient relative humidity, while Fig. 24.8 [36] shows the effect of the pH of the solution in which the measurements were made.

In the section on intrinsic strength, we showed the effect of water on the strength of silica fibers. In Fig. 24.7, we show in detail the effect of changes in water concentration or activity (relative humidity) on the strength measured on a time scale of approximately 10 seconds. As shown earlier, during the time of measurement, the strength has actually decreased from its inert value of approximately 14 GPa (or ~20% strain) to a value of the order of 5 GPa. As the relative humidity is increased, the strength decreases continuously, from about 6 to 5 GPa.

The behavior illustrated in Fig. 24.7 deals with the effect of relative humidity. In the case of aqueous solutions, there is also an effect of the pH of the solution and this is shown in Fig. 24.8. In aqueous environments, reaction with hydroxyl ion is rapid compared to reaction with molecular water, explaining the sensitivity to pH.

24.3.1.4 Tension

Light-guide fibers that are manufactured today show very high and very consistent tensile strengths. Figure 24.9 [37] shows a Weibull probability plot

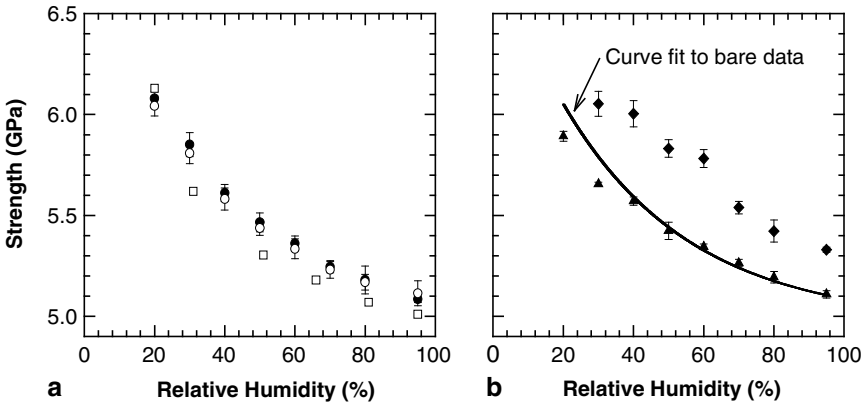

Figure 24.7 Effect of relative humidity on the strength of light-guide fibers. (a) data for ○ bare fibers, ● acrylate coated fibers, and □ silicone coated fiber. (b) data for ▲ polyimide and ◆ silicone coated fibers compared to the bare data. (Data used, with permission, from reference [35].)

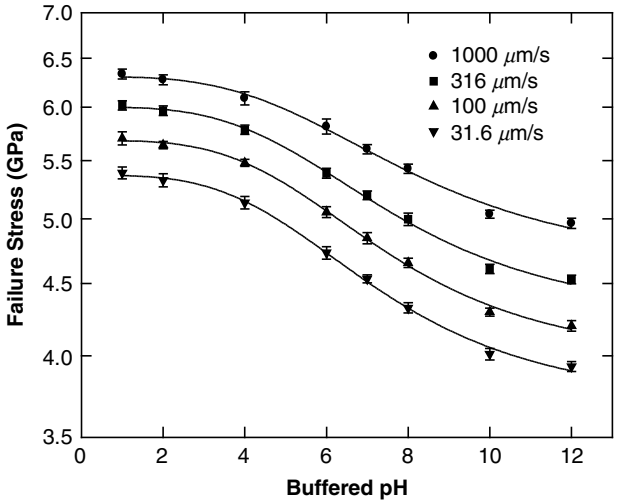

Figure 24.8 Effect of pH on the strength of light-guide fibers (data used, with permission, from reference [36]).

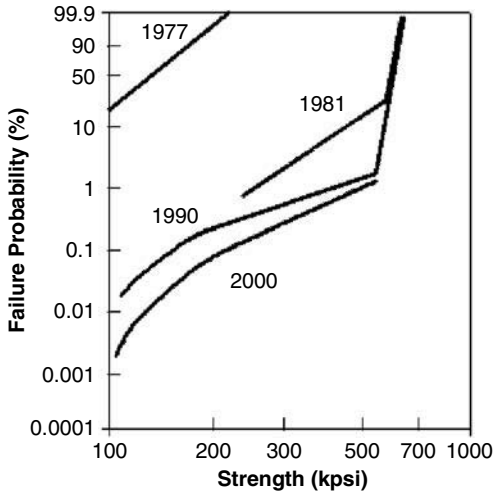

Figure 24.9 Weibull plot of strength of 20-m gage length of silica light-guide fibers showing how improvements have been made over the years [37]. (1 kpsi = 6.9 MPa.)

of the tensile strength of light-guide fibers tested in tension for a 20-m gage length representing the improvements in strength over the years. For simple uniaxial tension,

$$\sigma = \frac{L}{\pi r^2}, \tag{24.5}$$

where σ is the tensile strength, L is the applied axial load, and r is the fiber radius. Therefore, in tension, the stress for a given load is higher when the fiber has a smaller diameter. Table 24.2 shows what axial loads are required to generate a range of values of stress for several fiber diameters in the range of practical interest.

In Fig. 24.9, it can be seen that the curve is bimodal. It has been shown that the very narrow high-strength mode is the "intrinsic" strength of the fiber under the test conditions. That is, the lengths of fibers showing this high uniform strength are flaw free. If such breaking is accomplished in the absence of water (say in vacuum or at 77 K), the strength of such flaw-free fibers is approximately 14 GPa. Under normal ambient conditions, the measured strength is time dependent and is approximately 5.5 GPa at room temperature and tested in 10 seconds (Fig. 24.9). There should be no slope to this curve. However, while very high values of the Weibull slope, m (which correspond to a narrow distribution, see later discussion), can be measured in short lengths, many experimental factors contribute to the more moderate value of $m \sim 50$. The lower strength broader distribution reflects a variety of "manufacturing" defects or flaws. These flaws act to reduce the strength of the fiber by acting as stress-concentrators according to Eq. (24.3).

The exact nature of the failure probability–strength curve obviously depends on a number of factors but is represented reasonably by the lowest curve in Fig. 24.9 for good current manufacturing practices. As is seen later, this probability curve depends on the gage length tested.

Table 24.2

Axial loads (for tensile loading) and bending radii (for flexural loading) that result in a given stress for fiber diameters of 125 and 80 μm

Stress (GPa)	Tensile load (N)		Bend radius (mm)	
	125-μm fiber	80-μm fiber	125-μm fiber	80-μm fiber
0.2	2.5	1.0	22.6	14.5
0.5	6.1	2.5	9.1	5.8
1	12.3	5.0	4.6	3.0
2	24.5	10.1	2.4	1.5

The bend radii are calculated using Eq. (24.2) with $E_0 = 72$ GPa and $\alpha = 2.125$ (i.e., fused silica)

24.3.1.4.1 Weibull Statistics

As we have discussed, the strength of brittle materials is controlled by the presence of stress concentrating defects. Such defects are distributed in size/severity, nature, position, and orientation. As a result, the average measured strength of a set of specimens depends on the specimen size because larger specimens are more likely to contain larger defects and so are expected to be weaker on average. Weibull's weakest link theory for brittle fracture [18] assumes that failure is caused by the most severe defect and provides the following result for how the cumulative probability of failure by an applied stress σ, $F(\sigma)$, is related to σ and the length of the fiber, L,

$$F(\sigma) = 1 - \exp[-Lf(\sigma)] \tag{24.6}$$

or

$$\ln\ln\frac{1}{1-F} = \ln L + \ln f(\sigma) \tag{24.7}$$

where $f(\sigma)$ is a monotonically increasing function of σ. $f(\sigma)$ is not known *a priori,* but an empirical power law is ubiquitously assumed, which corresponds to the Weibull distribution:

$$f(\sigma) = (\sigma/\sigma_0)^m, \tag{24.8}$$

where m is the Weibull shape parameter (an inverse measure of distribution width) and σ_0 is the Weibull scale parameter, which is a measure of centrality of the strength distribution. This results in the well-known Weibull distribution. Equation (24.7) then becomes

$$\ln\ln\left(\frac{1}{1-F}\right) = \ln L + m\ln\sigma - m\ln\sigma_0. \tag{24.9}$$

Considering the failure of specimens with two lengths, L_1 and L_2, the applied stresses that give the same probability of failure, σ_1 and σ_2, are related by

$$\ln\frac{\sigma_1}{\sigma_2} = \frac{1}{m}\ln\frac{L_2}{L_1}. \tag{24.10}$$

Equation (24.10) is valid for any value of F, so it is valid for the mean strength, median strength, or indeed any other percentile. Therefore, as expected, longer specimens are weaker than short ones.

This formalism shows how the strength depends on specimen length. However, it results in σ_0 having the strange units of [stress] $\times$ [length]$^{1/m}$. σ_0 can be given the expected units of stress in several ways, but the simplest is to drop the length dependence in Eq. (24.9) to give

$$\ln\ln\left(\frac{1}{1-F}\right) = m\ln\sigma - m\ln\sigma_0. \tag{24.11}$$

For a given set of specimens, the length dependence of strength is ignored and the strength data are interpreted in terms of Eq. (24.11); when other specimen lengths are considered, Eq. (24.10) is used. Equation (24.11) may be visualized using a "Weibull plot," which is a graph of $\ln\ln [1/(1-F)]$ versus $\ln\sigma$, which, if the strength data are described by a Weibull distribution, is a straight line of slope m and intercept on the horizontal $\ln\sigma$ axis of $\ln\sigma_0$. σ_0 is the 63rd percentile.

If the strengths are measured of specimens of length L_1, then the expected strengths for specimens of length L_2 can be calculated using Eq. (24.10). Graphically, Eq. (24.10) represents a sideways shift on the Weibull plot by an amount $\ln(L_2/L_1)/m$ or equivalently a vertical shift along the probability axis of $\ln(L_2/L_1)$. An example of a Weibull plot is shown in Fig. 24.10 [38]. The right-hand axis is linear in $\ln\ln [1/(1-F)]$, while the left-hand axis is the actual failure probability and is nonlinear. The shift in the strengths with test length in Fig. 24.10 is illustrated in Fig. 24.11 where the mean strength is shown schematically as a function of gage/test length [38].

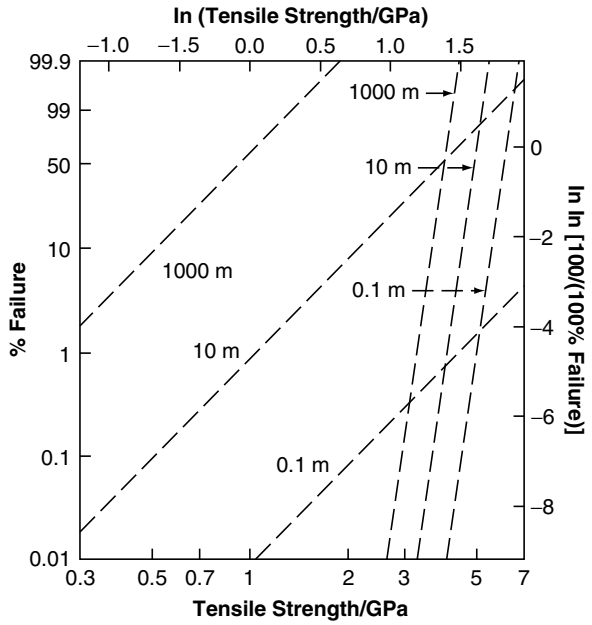

Figure 24.10 Schematic of Weibull plots for different fiber test lengths: Dashed lines are for a broad low strength distribution and solid lines are for a narrow high strength distribution. (Modified, with permission, from reference [38].)

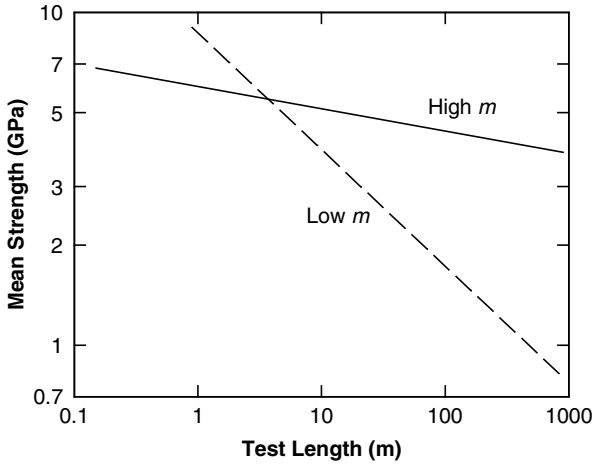

Figure 24.11 Schematic of mean strength versus test length for a narrow low Weibull modulus, *m* (solid line), and a broad high Weibull modulus (dashed line) strength distributions. (Modified, with permission, from reference [38].)

24.3.1.5 Bending

Light-guide fibers are often deployed in a bent configuration. The fundamental equation for the bending of a fiber into a circular loop is the following:

$$\varepsilon = \frac{r}{R}, \tag{24.12}$$

where ε is the maximum tensile strain that is on the outside of the bend, r is the radius of the fiber, and R is the bend radius or the radius of curvature. Therefore, for the same maximum strain (or stress), the minimum permitted bend radius is proportional to the fiber diameter. As a result, for fiber of a given strength subjected to primarily bending stresses, employing thinner fiber permits bending to tighter radii. In contrast, for fiber subjected primarily to axial tension, thicker fiber can withstand higher axial loads (Eq. [24.5]).

As already mentioned, testing of optical fibers is often carried out in two-point bending. This is because of the simplicity of the testing and because the very short length tested avoids manufacturing defects. The application of a bending stress will result in failure when the tensile stress on the outside of the bend reaches the failure stress. While Eq. (24.12) is appropriate for a circular loop of fiber, the strain in two-point bending is approximately 20% higher. Because the fiber will fail when the stress and not the strain reaches a critical value, the stress must be calculated from the bending strain. This is done by multiplying the failure strain by Young's modulus at this strain. The strain dependence of Young's modulus must be accounted for as shown in Eq. (24.2).

Table 24.2 compares the axial loads for tensile loading and bend radii for bending that result in a range of stresses and for two fiber diameters in the range of practical interest.

24.3.2 Fatigue

We have noted that many glasses are weaker when measured in ambient conditions compared to measurements in "inert" environments, such as liquid nitrogen (77 K). The phenomenon causing this effect is termed *fatigue*. Most inorganic glasses show a time-dependent strength or delayed failure. This effect is apparent either on testing dynamically, when the measured strength is lower for slower stressing rates, or statically by applying a fixed load (stress), which eventually leads to failure, with the time to failure decreasing with increasing stress. At least in oxide glasses, the mechanism is the combined effect of stress and the hydrolysis of strained siloxane bonds at the "crack" tip by ambient moisture:

$$\equiv \mathrm{Si} - \mathrm{O} - \mathrm{Si} \equiv + \mathrm{H_2O} \rightarrow \equiv \mathrm{Si} - \mathrm{O} - \mathrm{H} + \mathrm{H} - \mathrm{O} - \mathrm{Si} \equiv . \qquad (24.13)$$

In nonoxide glasses, the mechanism is often not completely determined. Figure 24.12 [39] shows results of fatigue measurements over a rather extended time range. This is the result of the combination of a number of studies using various techniques. The combined results form a single curve.

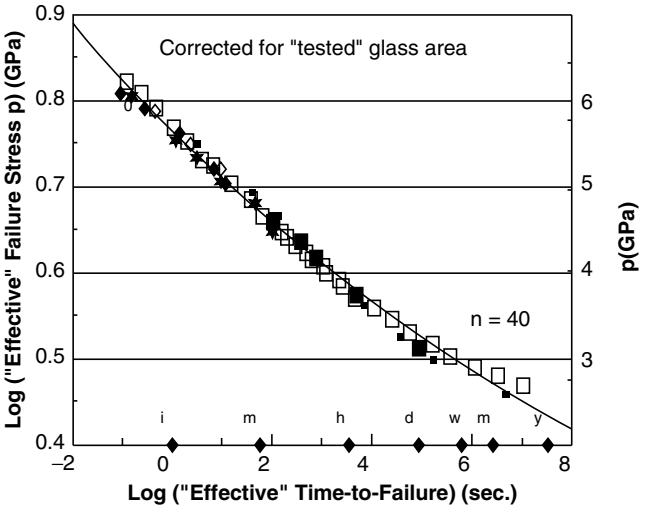

Figure 24.12 Compilation of fatigue data for silica light-guide fibers (used, with permission, from reference [39]).

A rough rule of thumb is that the long time strength is approximately one-third of the short time strength. A more complete analysis of a given fiber/device is, of course, ultimately required.

As indicated earlier, it is believed that the very strong short sections of light-guide fiber are flaw free. In spite of this, the generally applied model for fiber fatigue involves the slow propagation of cracks in the sample:

$$V = AK_{\mathrm{I}}^{n}, \tag{24.14}$$

where V is the crack growth velocity, K_{I} is the stress intensity factor, and A and n are empirical fit parameters. This equation appears to be appropriate whether the high or low strength behavior is considered. n is the stress corrosion susceptibility parameter. A higher value provides greater fiber reliability. It has been shown that because of the very severe dependence of the velocity on stress, it is difficult to tell whether the empirical power law or a physically more meaningful exponential form are more appropriate and thus the simpler power law is commonly used, primarily because of its mathematical convenience. The power law does, however, provide more optimistic predictions of reliability than exponential models.

Service conditions are usually assumed to have constant applied stress and under such "static fatigue" conditions the time to failure, t_f, is given by

$$t_f = \frac{2}{(n-2)AY^2}\left(\frac{\sigma_i}{K_{\mathrm{IC}}}\right)^{n-2}\frac{1}{\sigma^n} = B\frac{\sigma_i^{n-2}}{\sigma^n}, \tag{24.15}$$

where

$$B = \frac{2}{AY^2(n-2)}\frac{1}{K_{\mathrm{IC}}^{n-2}}, \tag{24.16}$$

and where σ is the service stress and σ_i is the inert strength (i.e., the strength that would be measured when no fatigue occurs). This is effectively the strength of the fiber at 77 K. This is rarely known, but for silica it is approximately twice the strength measured at room temperature in times of the order of seconds (i.e., the normally measured strength). Equation (24.15) shows how the failure times for two different applied stresses are related:

$$(t_f\sigma^n)_1 = (t_f\sigma^n)_2. \tag{24.17}$$

For both high and low strength silica fibers, it is assumed with reasonable justification, that $n \approx 20$.

For strength measurement using a constant stress rate, $\dot{\sigma}$, the failure stress, σ_f, is given by

$$\sigma_{f,\dot{\sigma}}^{n+1} = \frac{2(n+1)\dot{\sigma}}{AY^2(n-2)}\left(\frac{\sigma_i}{K_{\mathrm{IC}}}\right)^{n-2} = (n+1)B\dot{\sigma}\sigma_i^{n-2}. \tag{24.18}$$

Laboratory testing that has been accelerated by using aggressive environments (high temperature, high water activity) has shown an additional strength reduction mechanism in addition to fatigue. This ''aging'' phenomenon must be considered because of its potential negative impact on reliability.

24.3.3 Aging

In the study of the strength and reliability of silica light guides, testing is often carried out under extreme conditions to accelerate the degradation and, thus, hopefully allow prediction out to longer times/lifetimes. When this was done early in the study of silica light-guide fibers, an effect that had not really been known earlier was discovered in both aging and fatigue [40, 41]. If fiber is held for some time under no stress and subsequently strength tested, it is found that depending on the condition of holding, or aging, the strength may have degraded. This is now known as *zero stress aging,* or more simply *aging*. Figure 24.13 shows results of a rather long duration aging test of a polymer-coated silica fiber aged in distilled water at 25 °C and a shorter time test in 100 °C water [42]. As can be seen, for some prolonged period, no strength degradation occurs, but eventually rather precipitous strength degradation occurs. This effect has been shown to be present in fatigue as well and the time scale depends on the state of the water [43] (Fig. 24.14). The important fact to be learned from Fig. 24.13 [42, 44] is that the activation energy for the process responsible for this strength degradation is approximately 80 kJ/mol, the activation energy for the reaction of silica with water.

The model that has been used to describe this aging effect involves surface roughening. As we have discussed, glasses are essentially supercooled liquid glasses and, as such, contain both chemical and structural fluctuations. These fluctuations have different thermochemical properties, including water solubility and dissolution rate. These differences lead to roughening of the glass surface as shown in the atomic force microscopy (AFM) images in Fig. 24.15 when the surface is exposed to an aggressive environment [45]. This effect was studied in greater detail using a model system by Inniss et al. [27].

A more pronounced effect was shown in the borosilicates studied by France et al. [6] and is shown in Fig. 24.16. In this case, not only are these glasses less durable, but they show composition fluctuations that will contribute to the unequal solution rate effects. Such fluctuations have been shown in optical scattering studies.

The preceding discussion relates to the aging behavior of the pristine fiber strength, rather than the behavior of the occasional defects. Evidence suggests that aging weak defects in aggressive environments can lead to strength recovery

Figure 24.13 Effect of temperature on the aging of silica light-guide fibers (data used, with permission, from reference [42]). The ratio of the strength after aging to the strength before aging is shown as a function of the aging time in both 25 °C (■) and 100 °C (●) water.

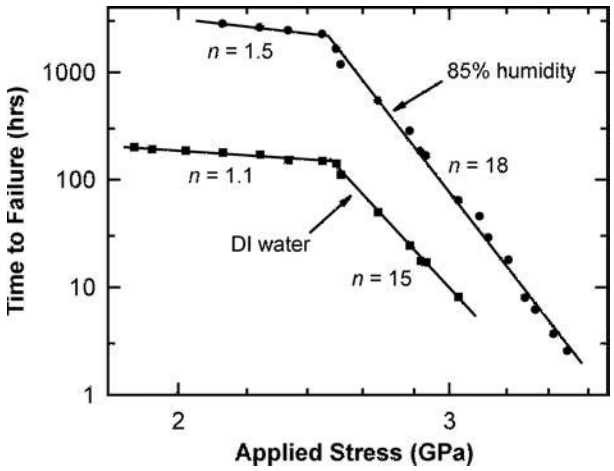

Figure 24.14 Effect of liquid water and water vapor on the static fatigue of silica light-guide fibers (data used, with permission, from reference [43]).

in much the same way as etching in hydrofluoric acid (a discussion of which is presented later). However, strength loss of the strong sections of fiber might be more important because the fiber might become too weak to handle along its entire length.

24.3.4 Nonsilicate Glasses

The measurement of the strength, fatigue, and aging of nonsilicate glasses has not been very extensive. The measurements have often been made in two-point bending and, therefore, usually not for long lengths of fiber. While this is valuable for the assessment of the measured strength relative to the theoretical strength, these are not necessarily practical or useful strengths. In this section, we discuss all of these properties in nonsilicate glasses.

24.3.4.1 Heavy-Metal Fluoride Glasses

The mechanical properties of HMF glasses are quite sensitive to the presence of liquid water, but not as sensitive to water vapor. The highest strengths for HMF glass fibers whose surface had been etched are approximately 1.4 GPa [46]; because the measurement was made in bending, the calculation of the failure stress depends on knowledge of the Young modulus. Carter [47] found

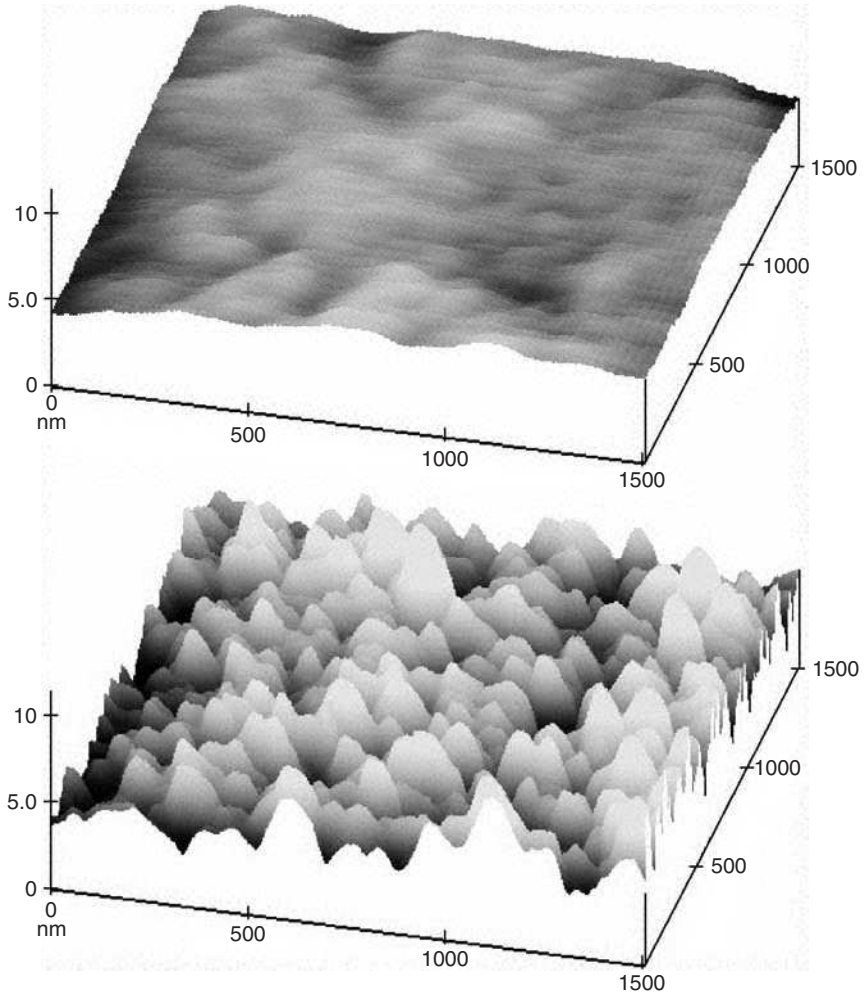

Figure 24.15 AFM images of the roughness which develops upon aging silica fibers–the upper image of the unaged surface while the lower image is from a fiber that had been aged for 168 hours in 90 °C pH 7 buffer solution (used, with permission, from reference [45]).

similar values and attributed the less than theoretical strength to the presence of bubbles and crystals. Her results (Fig. 24.17) illustrate the differences that may be seen in testing different fiber lengths.

Perhaps the most detailed study on fatigue and aging in HMF glasses is that of Colaizzi and Matthewson [48] who characterized glasses whose compositions included AlF_3 (Fig. 24.18).

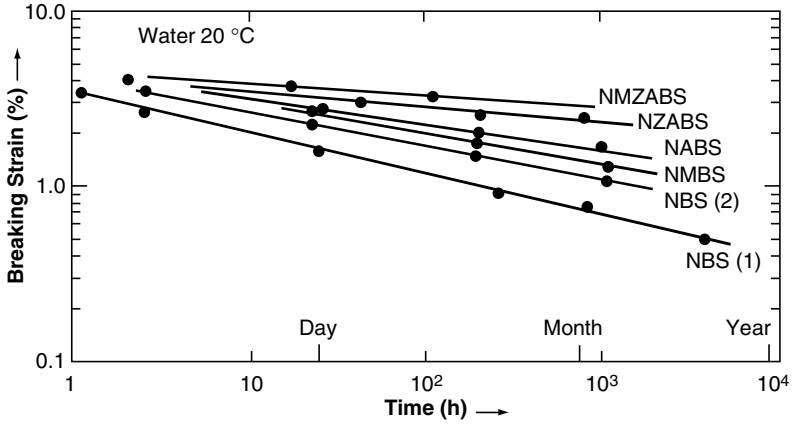

Figure 24.16 Aging of fibers of alkali borosilicate glasses of various compositions (used, with permission, from reference [6]).

24.3.4.1.1 Chalcogenide Glasses

Studies of the two-point bend strength of arsenic sulfide glass fibers as seen in Table 24.1 show the apparent approach to that theoretically expected strength, namely 1.5–2.5 GPa. Devyatkh et al. [49] published a value for strength under ambient conditions of approximately 1.2 GPa. Sanghera [50] (Fig. 24.19), measured about a half of that value (0.570 GPa) at room temperature, but a value of 0.854 GPa at 77 K (i.e., ~1.5 times greater than the room temperature strength). Applying this ratio to the data of Devyatkh et al. [49] would give an "inert" strength of approximately 2.4 GPa or $E/\sigma \sim 6$ for their fibers. In fact these data are presented as strength, although the measured values are actually failure strain. In the case of Devyatkh et al. [49], estimated strengths at 77 K amount to a failure strain of approximately 16%, very nearly that found for silica.

While the situation with respect to the fatigue and aging of silica and silica-based glasses is clearly due to the presence of water, the situation for chalcogenide glasses is not as clear; there is no clear-cut experimental evidence for the critical chemistry. Dianov et al. [51] give values of $n \sim 10$–20, but the scatter in the data (Weibull modulus, $m \sim 10$) leaves this in doubt. The data of Sanghera (Fig. 24.19) are interesting in this regard. Here, we see that the ratio of strengths at 77 K and room temperature is approximately 1.5, while the ratio of room temperature to metal-coated strength is approximately 5. One possibility we may suggest here is that the fatigue is due to the interaction of the glass with oxygen rather than water.

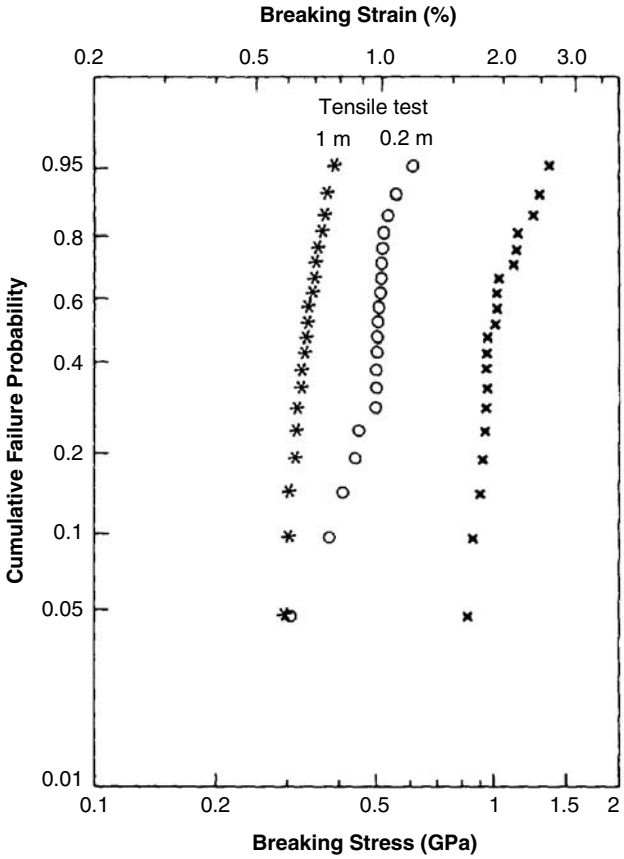

Figure 24.17 Weibull plot of the strength ZBLAN fibers measured in bending and in tension with test lengths of 0.2 and 1 m (used, with permission, from reference [47]).

24.3.5 Photonic Crystal or "Holey Fibers"

The only set of experimental results on photonic crystal (PC) fibers is that of Zhou et al. [52]. These workers have found that the two PC fibers they have studied, with respectively 90 and 6 holes, show breaking loads effectively 10 and 20% higher than that found for standard single mode fused silica clad fibers. When account is taken of the differences in cross-sectional area (3% and 0.4%, respectively), the strengths are 4.45, 5.0, and 5.4 GPa, respectively, for the standard single-mode fiber, 90-hole fiber, and 6-hole fibers. However, the experiments were not well controlled in that the three fibers had different

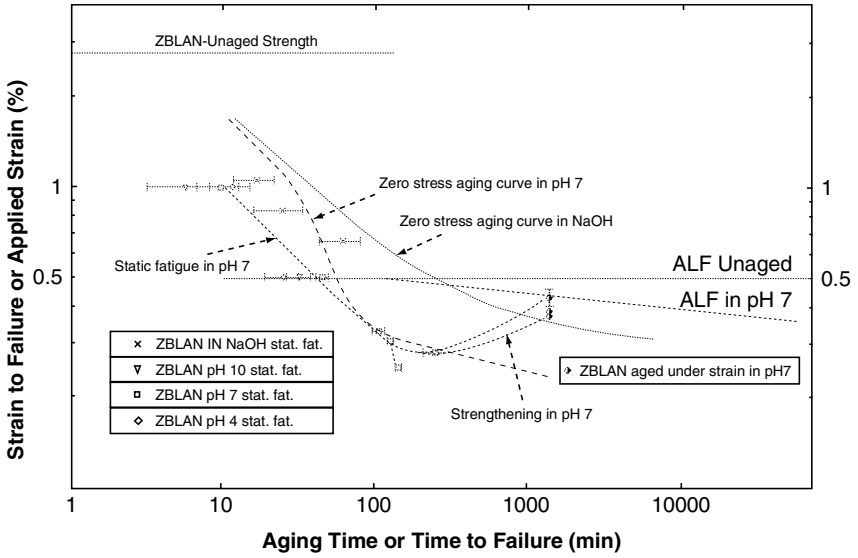

Figure 24.18 Compilation of fatigue and aging data for ZBLAN and aluminum fluoride-doped ZBLAN ("ALF") fibers (used, with permission, from reference [48]).

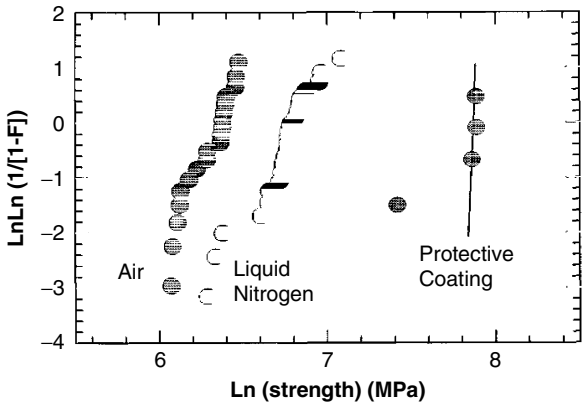

Figure 24.19 Effect of environment on the bending strength of As_2S_3 fibers (used, with permission, from reference [50]).

polymer coatings, so the difference in strengths might not be significant. Further, because the flaws causing failure are substantially smaller than the holes or the distance between the holes, the presence of the holes is not expected to have any effect on strength.

24.4 COATINGS

24.4.1 General Comments and Polymer Coatings

Very early in the development of the light-guide technology, it was clear that the pristine surface of the as-drawn fibers would have to be protected from mechanical damage by applying a thin polymer coating to isolate the fiber surface from any hard sharp particles in the environment. As their development progressed, dual coatings were developed; the inner compliant coating reduced the microbending losses, while the harder more abrasion resistant outer secondary coating made the assembly more robust. Contrary to much early literature, polymer coatings were found to be quite permeable to water [53]. It was found that penetration through typical coatings, which are approximately 60 μm thick is accomplished in times of the order of 1 hour or less. Therefore, one must still expect strength degradation from both fatigue and aging. The details of the coating chemistry are apparently of importance to the aging behavior of the fiber and perhaps less so to the fatigue behavior, but no detailed explanation has yet been given.

24.4.2 Metal Coatings

As indicated earlier, the polymer coatings that have been applied to light-guide fibers have been shown to be quite permeable to water, so once steady state has been attained, the fatigue and aging behavior of coated and bare fibers are similar. It is natural, therefore, that a fair amount of early work was done on coatings that were hermetic (i.e., those that would isolate the fiber surface from water). Figure 24.20 [54] shows that the use of a metal coating can result in a strength that is similar to that obtained at 77 K, that is, the inert strength. The results in Fig. 24.20 are given as failure strength and should probably be corrected because they were taken in two-point bending and Eq. (24.2) was used to calculate failure stress with $\alpha = 3$ instead of the value of $\alpha = 2.125$ appropriate for bending. However, Eq. (24.2) has only been verified for strains up to approximately 6% and is incorrect for the failure strains seen in Fig. 24.20.

24.4.3 Inorganic Coatings

Many inorganic coatings have been tried, but the best has been found to be carbon, even though the behavior is complicated and variable. Figure 24.21 [55] illustrates the effect of draw speed on the strength and fatigue parameter, n. This

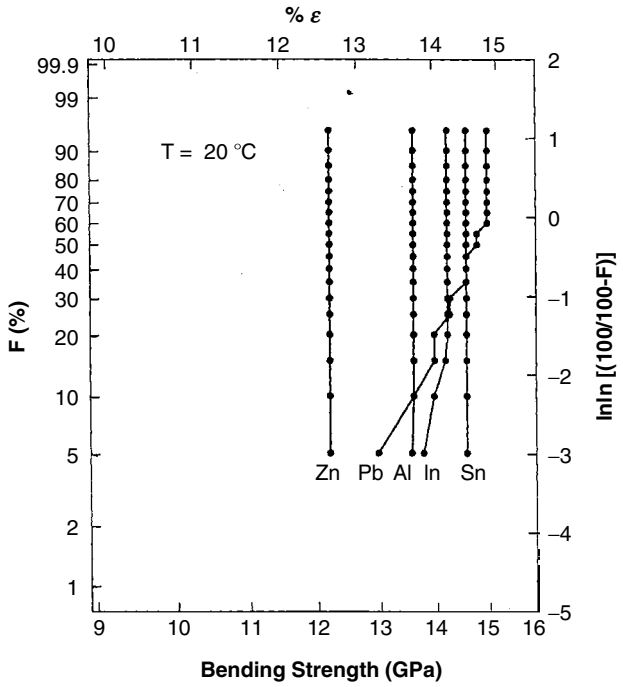

Figure 24.20 Effect of melt-applied metal coating on the bend strength of silica light-guide fibers (used, with permission, from reference [54]).

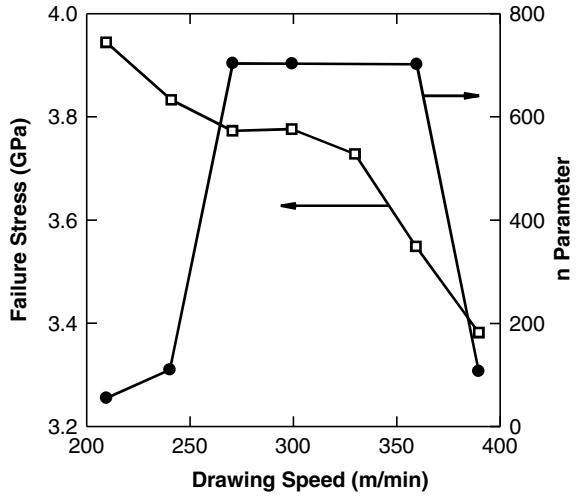

Figure 24.21 Effect of fiber draw speed on the resultant fiber strength and fatigue parameter, *n*, for carbon coated silica (data used, with permission, from reference [55]).

is an effect connected primarily to the thickness of the coating. However, it is known that the coating ''composition,'' thickness, and roughness influence the strength, fatigue (water permeability), and hydrogen permeability [56].

24.5 HANDLING AND POST-DRAW PROCESSING

In our earlier discussions, we considered short time fiber strength, long time fiber strength, fatigue and aging, all things that must be considered in the design of the system under consideration if some reasonable assumptions about the strength of the starting fiber are made. On the other hand, some type of fiber handling and processing are very often required in the fabrication and assembly of any given device. In this section, we describe some specific operations that may introduce unpredictable damage. By keeping in mind certain factors that can affect the strength of the fiber as a result of such processing, it should be possible to minimize both these strength reductions and reduce unexpected reliability consequences.

24.5.1 Fiber Stripping

All-silica light-guide fibers have a coating (usually a polymer) applied in-line during drawing to protect the glass surface from mechanical damage. Use of fibers in practice very often necessitates the removal of this coating. Three general techniques can be used to accomplish this: mechanical, chemical, or thermal.

While stripping in the field most commonly uses a tool similar to diagonal cutting wire strippers where the stripping hole is somewhat larger than the fiber diameter, this will inevitably lead to a strength reduction due to the sort of mechanical damage illustrated in Fig. 24.22 [57]. While the strength reduction can be considerable in some cases, in general, there are still substantial lengths that have been left undamaged. Knowing this, it is possible to employ the very simple and quick mechanical stripping technique in conjunction with a proof-testing procedure to guarantee a desired strength.

Other techniques have been employed that remove the coating with less surface damage and, therefore, with less strength reduction. The technique that has been found to produce the cleanest surface with no damage due to the process itself is chemical stripping using hot ($\sim$200 $^{\circ}$C) concentrated sulfuric acid [58]. This process effectively removes most polymer coatings in a few seconds, producing a ''clean'' surface. It has been shown that by careful handling and stripping in this way, no strength reduction is observed [59]. In certain cases, soaking in acetone or methylene chloride may be used. These chemicals

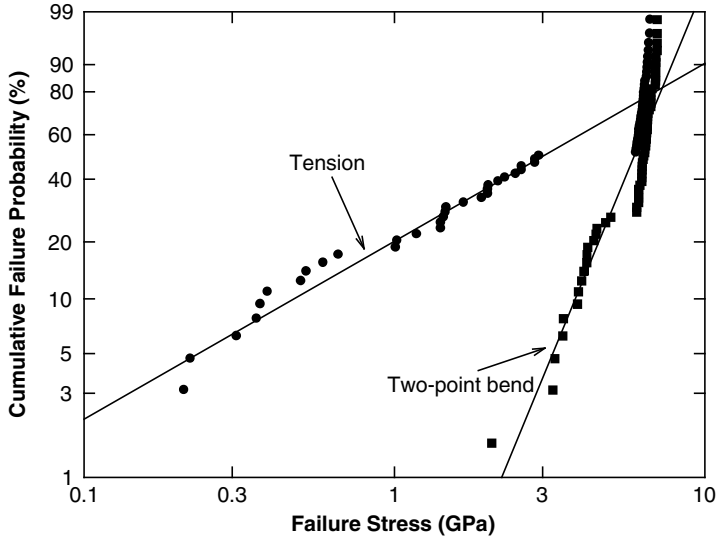

Figure 24.22 Weibull plot of the strength of mechanically stripped fiber measured in tension (●) and bending (■) (data used, with permission, from reference [57]).

cause swelling of the coating, which may then be stripped off with no strength reduction. There are also a number of thermal strippers available on the market, which can produce quite acceptable stripped fiber strengths.

Park et al. [60] described an interesting and quite different approach. Their stripping technique makes use of the fact that the primary and secondary polymer coatings on dual-coated fiber have distinctly different properties. By rapid local heating, the compliant primary coating will rapidly expand and effectively "explode" the more brittle primary coating with a resultant rather small decrease in fiber strength.

24.5.2 Fiber Cleaving

As discussed earlier, in the fracture of inorganic glasses, we are dealing with failure in a brittle manner. This results in a fracture surface that is generated by the propagation of a crack perpendicular to the axis of the applied stress. If the applied stress is appropriate and the crack is of the right size and orientation, the crack will propagate such that a smooth "mirror" fracture surface is generated perpendicular to the fiber axis. The details of this process are given in the section on fractography. Here, we simply illustrate the type of fracture surfaces that can be developed. Figure 24.23 [61] shows micrographs of fracture surfaces. In each case, the fracture was generated by a scratch at the bottom surface (i.e., the

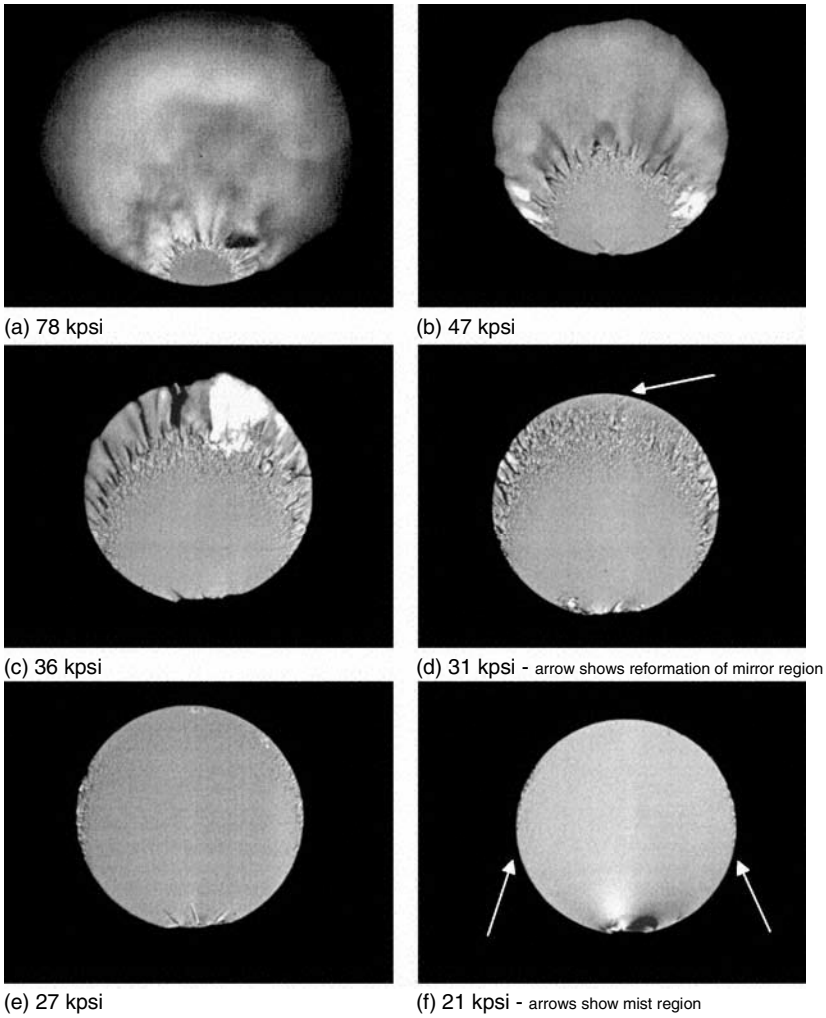

Figure 24.23 Fracture surfaces of fibers that broke at a range of failure stresses (a) 0.538 GPa, (b) 324 MPa, (c) 248 MPa, (d) 214 MPa, (e) 186 MPa, and (f) 145 MPa (used, with permission, from reference [61]).

6 o'clock position). Figure 24.23a–f shows the fracture surface for increasingly large scratches, and consequently the fracture stress, as indicted by each micrograph, becomes less. It is seen that the smooth region/mirror becomes larger as the strength decreases. The objective of a good cleave is to have this mirror be the size of the entire fiber so that good mating is achieved. The details of

fractography are described later. Care must be taken that a simple cut is made and that there is not extensive damage to the fiber surface.

24.5.3 Splicing

The joining of two sections of optical fiber can be done either mechanically or by fusion splicing. In mechanical splicing, the ends of the two fibers are joined by gluing them inside a sleeve or ferrule. While this technique is simple and rapid, it is bulky and not particularly robust. For high-quality, high reliability work, especially for undersea use, fusion splicing is often employed. Figure 24.24 illustrates some very early splicing work [62]. This shows the importance of avoiding damaging the fiber during stripping or subsequent handling. In the case of both splicing and tapering, some portion of the fiber is re-heated. In the center region of either a splice or a taper, the fiber is completely melted and, thus, when cooled will be expected to have original perfect fiber strength. At intermediate positions along the fiber, the maximum temperature will be intermediate between the melting temperature and room temperature. In some

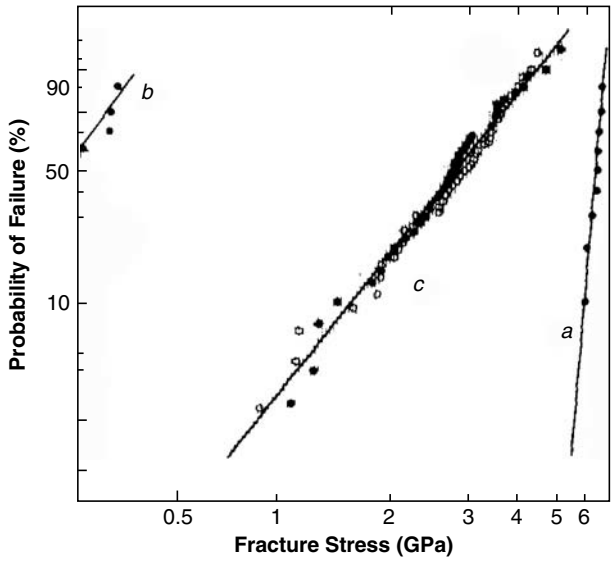

Figure 24.24 Early strength results for fusion splices: (a) original fiber strength, (b) coating mechanically stripped, and (c) coating chemically stripped (used, with permission, from reference [62]).

of these regions, the strength degradation due to the interaction of the fiber surface with water in the atmosphere will be rapid enough to cause strength degradation during the processing time. Figure 24.25 shows later work by Krause [63]. Here, it is shown that by careful stripping and by adhering to appropriately "clean" conditions, splices showing very little strength degradation can be obtained, while if in addition to "clean" conditions, the conditions are also "dry" (accomplished by the use of a H_2/Cl_2 torch), essentially no strength degradation is suffered. While this is often not feasible in practice, strengths approaching those obtained under these ideal condition can be achieved.

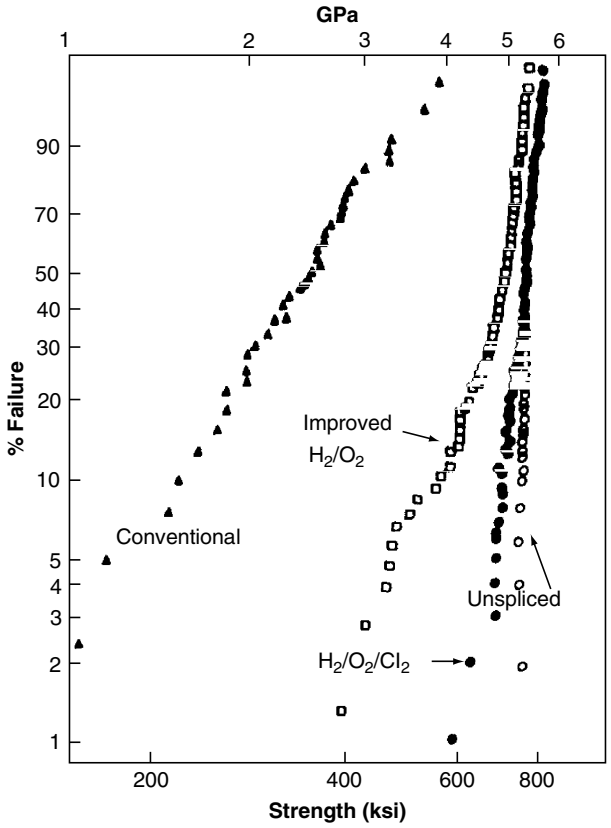

Figure 24.25 Weibull plot of the strengths of fusion splices made using various methods (1 ksi = 6.9 MPa) (used, with permission, from reference [63]).

It should be kept in mind that the temperature gradient, which necessarily accompanies any such heating of a portion of the fiber, such as in tapering or thermal lensing, may lead to substantial strength degradation by the interaction of the hot surface with moisture described earlier.

24.5.4 Polishing

Grinding and polishing of the ends of fibers involves many complicated and poorly understood processes. In the grinding process, sharp hard particles scratch the glass surface resulting in gouges and cracks. Some of these cracks cause chipping of the surface and thus removal of some of the glass. Grinding is used to rapidly approach the final desired size and shape. The final shape and surface quality are produced by polishing. Polishing is similar to grinding except that much finer abrasive particles are used. In each of these processes, a series of decreasing abrasive particle sizes is employed so that the damage created in one step is removed in the next step. It is important that the abrasive used in one step be removed before the next step. Polishing has been shown to be a combination of mechanical and chemical processes, so the appropriate choice of both polishing material and size is important.

24.5.5 Soldering/Pigtails

Fibers often need to be soldered into packages, many times to achieve hermeticity or to precisely maintain dimensional stability. It would seem that the use of the very strong melt-coated fibers described earlier would be the first choice. While this is sometimes the case, in most cases, more or less standard metallization processing is used using—for instance—reactive metals such as Ti or Cr, which are evaporated or sputtered onto the glass surface and covered with a solderable and oxidation-resistant final layer. While this process provides good adherence of metal to glass, the resulting assembly is usually rather weak, presumably due to the strength reduction accompanying the sputtering of the Ti or Cr layer. Little detailed work has been published regarding the mechanism of strength reduction is such systems; it would seem reasonable to attribute the weakening to the reaction of the sputtered metal with the perfect glass surface. In the case of a silica fiber coated with aluminum by the melt process, high fiber strength, good adherence of metal to glass, and good joint pull strength have been achieved (Fig. 24.26) [64]. While not completely understood, although there is apparently interaction between the silica surface and the aluminum coating, the strength is recovered upon chemically stripping the aluminum [65].

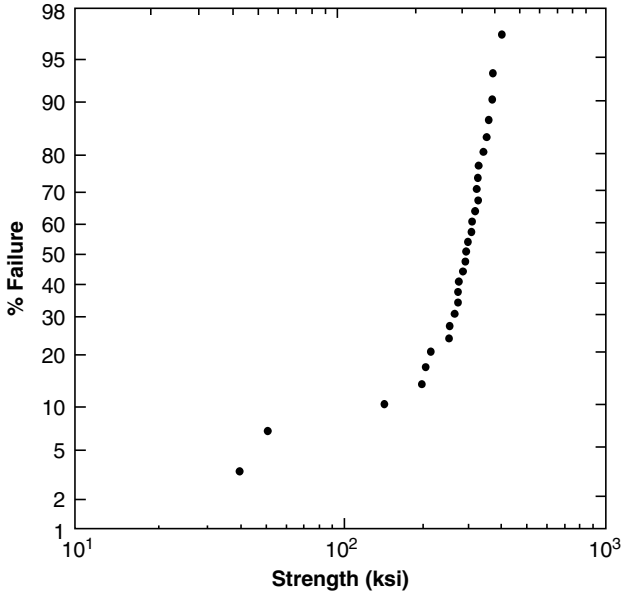

Figure 24.26 Strength of solder joints to aluminum-coated fiber (1 ksi = 6.9 MPa) (used, with permission, from reference [64]).

24.5.6 Recovery of Handling Damage: Etching

The use of hydrofluoric acid (HF) for the etching of glass surfaces has been practiced commercially for many years. Proctor et al. [66] found that etching of damaged commercial soda-lime–silica glass rods resulted in substantial recovery of strength. In the case of silica rods, the recovery was not nearly as great; the maximum room temperature strength recorded was approximately 2.5 GPa. Vitman et al. [67] partially recovered strength of an abraded fiber. Miyama et al. [68] etched silica light-guide splices and were able to increase the mean fiber strength from 0.8 GPa to approximately 2 GPa. Kurkjian et al. [69] showed that etching of high-strength silica light-guide fibers resulted in a decrease in normal room temperature two-point bending strength from 5.5 GPa to a steady-state plateau value of approximately 3.5 GPa (Fig. 24.27). It was suggested that the smooth perfect fiber becomes roughened by the acid etch and that the roughness acts as stress concentrators as described earlier in the section on aging. Thus, although additional work is needed, we suggest that by appropriate etching of fibers damaged by handling abrasion or other mechanisms, strength increases to at least 3.5 GPa should be possible. Of particular practical importance, Kurkjian et al. [69] found that the weakening of the perfect fiber was accomplished both

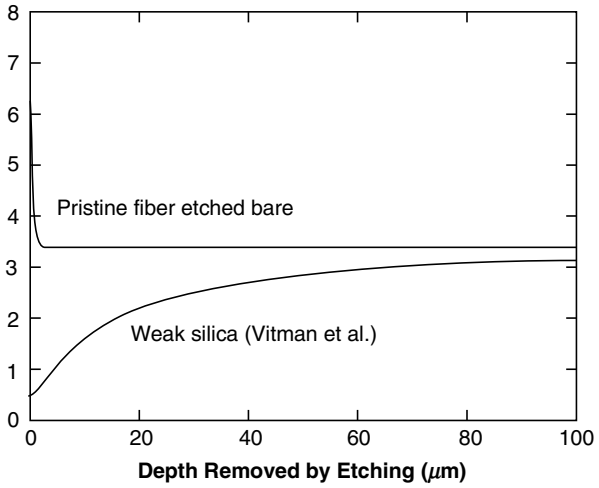

Figure 24.27 Strength increase in weak fiber and strength decrease in flawless fiber on exposure to HF.

with bare fibers and with coated fibers. Thus, it would be expected that strengthening could also be accomplished by etching through the coating, which has been found [70].

24.6 FRACTOGRAPHY

A very useful practical tool is fractography. This is the microscopic study of fracture surfaces. Such studies can give valuable information about the stress level at which a fiber failed, the distribution of failure stress (tension/bending/torsion), and can give an indication of the reason for failure. Figure 24.23 illustrates the features that may be seen on a typical fracture surface. At the early stages of propagation, a crack will grow slowly and during this time will produce fracture surface that is quite smooth; this region is the "mirror." The crack continuously increases in velocity, gradually approaching its limiting velocity (approximately one-third the longitudinal sound velocity) at which point the excess energy begins to be taken up by the creation of extra fracture surface; the surface roughens (the "mist" region) and at higher speeds produces steps in the surface (the "hackle" region).

It has been empirically found that the radius of the mirror region, r_m, is directly related to the stress at failure, σ, by

$$\sigma = \frac{A}{r_m^{1/2}}, \tag{24.19}$$

where A, the mirror constant, is a parameter found empirically. It has been found that for all glasses considered here, the ratio of the mirror radius, r_m and the original flaw size, c, is approximately 0.1. From Eq. (24.19), it can be seen that A has the units of stress intensity and is essentially proportional to K_{IC}. If $c \sim r_m/10$, then, $K_{IC} \sim 0.4A$.

24.7 PROOF-TESTING AND RELIABILITY

As we have discussed earlier, the majority of the length of fiber has an extremely high strength, but occasional weak defects are encountered, which are introduced during manufacturer. These weak defects control the practical reliability of fiber that is of useful length (i.e., more than a few millimeters). Review of Eq. (24.9) for the Weibull strength distribution shows that even for very low applied stress, σ, there is a small but finite probability of failure, F. Mechanical reliability can only be completely ensured if the applied stress is actually zero, which cannot be achieved in practice, especially for applications in which the fiber is bent. The situation is greatly improved by "proof-testing"—which involves applying a short pulse of stress to the entire fiber length—the weakest defects will fail under the proof stress and so are eliminated. If the fiber breaks, it can be discarded or spliced (followed by proof-testing of the splice, of course). The resulting lengths of fiber will have a certain minimum assured strength after proof testing. Choice of the proof stress is a compromise: A high proof stress gives fiber with a high ensured strength but increases the frequency of proof failures and hence decreases yield. Lowering the proof stress improves yield but reduces the minimum strength. For silica fiber in telecommunications applications, the proof stress is typically 700 MPa (100 kpsi).

Proof-testing of long lengths of fiber is normally performed using a continuous tester in which the fiber is fed around a pair of pulleys that apply a given tensile load to the section of fiber between them. While useful for long lengths of fiber, this technique is not suitable for short lengths. In that case, the fiber is usually proof-tested by passing it through a series of rollers that bend the fiber in several directions so the entire surface of the fiber experiences a stress close to the maximum bending stress.

While the idea of proof-testing is simple, in practice it is complicated by fatigue. Firstly, proof-testing is conducted in ambient environment, so the surviving fiber has lost some strength during proof cycle. This is a minor effect, and because the weakest fiber is removed, the average strength of the surviving fiber is increased by proof-testing. Secondly, proof-testing ensures a minimum strength, which is the strength immediately after proofing (i.e., the minimum inert strength, σ_i, is the proof stress, σ_P). As a result, if the strength of lengths of proof-tested fiber is measured, fatigue during the measurement means that some

of the strengths are actually lower than the proof stress, although this occurrence is rare. Thirdly, the proof stress cannot be removed instantaneously so that fatigue occurs during the unloading phase. As a result, the minimum ensured strength is a little lower than σ_P. Crack growth during unloading is minor and is suppressed by unloading from the proof stress as quickly as possible. These three effects have been studied in detail and reliability models have been developed.

24.7.1 Minimum Strength Design

The most common and conservative approach to reliability modeling is known as the "minimum strength design." Here, the maximum applied stress is limited to some fraction of the minimum fiber strength, usually taken to be the proof stress. With this approach, one assumes that the length of fiber under stress is no weaker than the proof stress. This is appropriate in applications in which many kilometers of fiber are stressed or where the fiber has been weakened by handling events where the protective coating has been removed, for example, fusion splicing. For silica-clad optical fiber with a value of the stress corrosion parameter, $n \sim 20$, the allowable applied stress is shown in Fig. 24.28 for three common stress events. One is allowed to stress fiber to approximately one-fifth the proof stress for long-term events, one-third the proof stress for installation events lasting hours, and one-half the proof stress for short-term processing stresses. These guidelines are shown in terms of bend radius in Fig. 24.29. Assuming the typical proof stress of 700 MPa, the allowable bend radius for, say, fiber stranded about a central member in a cable is 32 mm. The maximum allowable tensile stress during installation of an aerial cable is 230 MPa for the same fiber. Pulleys used for guiding fiber during processing should be no greater than 25-mm diameter.

24.7.2 Failure Probability Design

In splice enclosures and many photonic device applications, relatively short lengths of fiber are permanently coiled and stored. As shown earlier, the probability of encountering a flaw in a short length of today's fiber is low. Thus, a failure probability design methodology is appropriate in these situations. A general rule of thumb is that one can consider a failure probability design for deployed lengths of less than a kilometer.

Failure probability is incorporated into Eq. (24.15) through the inert strength, σ_i,

$$t_f = B(F\{\sigma_i\})^{n-2}\ \sigma_a^{-n}. \tag{24.20}$$

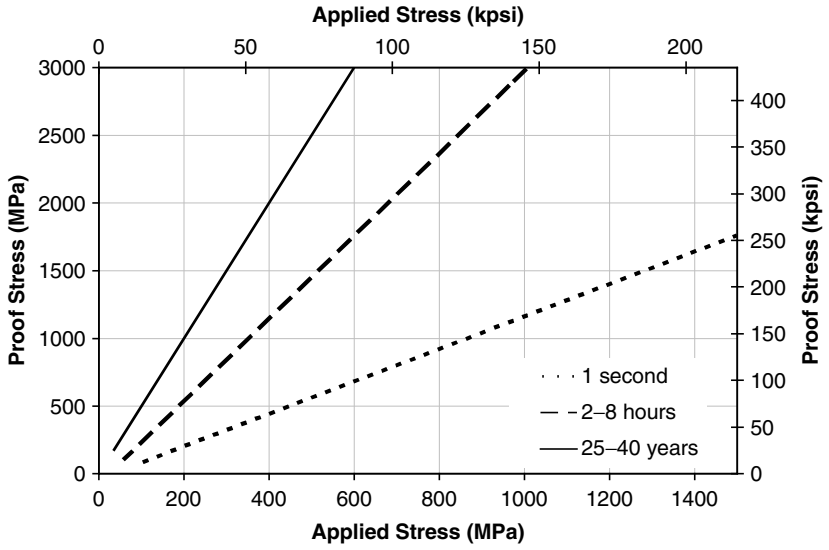

Figure 24.28 Allowable stress as a function of proof stress for processing (1 second), installation (hours), and in-service (years) stress events.

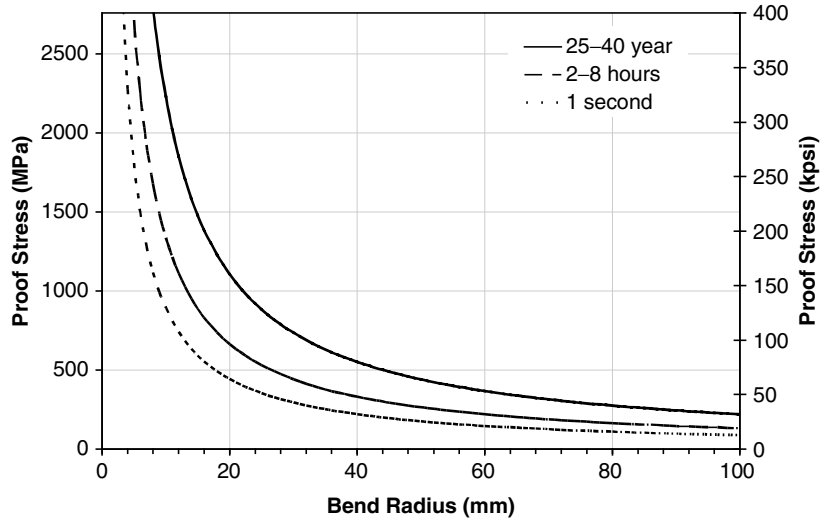

Figure 24.29 Allowable bend radius for common stress events.

The strength distributions, such as those shown in Fig. 24.9, can be directly substituted into Eq. (24.20), provided one accounts for the fatigue that naturally occurs when testing in air [71]. When such modeling was being developed, it was

recognized that one should account for fatigue during processing events like proof-testing and in-service life. The Telecommunications Industry Association has captured these developments into a reliability guideline based on the power law crack velocity model [72]. One of the most notable contributions is that of Mitsunaga et al. [73] where field failure probability is estimated from knowledge of the proof-testing conditions and the proof test break rate, N_P,

$$F = 1 - \exp\left(-N_P L \frac{m}{n-2} \frac{\sigma_a^n t_s}{\sigma_P^n t_P}\right), \tag{24.21}$$

where L is the length of fiber, σ_a is the applied stress in service which is applied for a service life t_s, σ_P is the proof stress which is applied for a time t_P. The Weibull modulus, m, is that of the pre–proof-test strength distribution. This model assumes that the distribution of flaws surviving proof-testing can be estimated from those failing proof-testing.

ACKNOWLEDGMENTS

We thank G. Scott Glaesemann of Corning, Inc., Corning, New York, for helpful comments and especially for contributions to the section on proof-testing and reliability.

REFERENCES

[1] Varshneya, A. K. 1993. *Fundamentals of Inorganic Glasses*. Academic Press, New York.
[2] Baikova, L. G. et al. 1967. Nature of the damage of high-strength glass and possibilities of protecting glass. *Sov. Phys. Sol. State* 9(2).
[3] Semjonov, S. L. and C. R. Kurkjian. 2001. Strength of silica optical fibers with cube corner indents. *J. Non-Cryst. Solids* 283/1-3:220–224.
[4] Pharr, G. M. et al. 1993. Measurement of fracture toughness in thin films and small volumes using nanoindentation techniques. In: *Mechanical Properties and Deformation Behavior of Materials Having Ultra-fine Microstructure* (M. Natasi, ed.), pp. 449–461. Springer, Berlin, Germany.
[5] Koizumi, K. et al. 1974. New light focusing fibers made by a continuous process. *Appl. Optics* 13:255–260.
[6] France, P. W. et al. 1983. Strength and fatigue of multicomponent optical glass fibres. *J. Mat. Sci.* 18:785–792.
[7] French, W. G. et al. 1975. Glass fibers for optical communications. *Annu. Rev. Mat. Sci.* 5:373–394.
[8] Lines, M. E. 1994. Can the minimum attenuation of fused silica be significantly reduced by small compositional variation? 1. Alkali metal dopants. *J. Non-Cryst. Solids* 171:209–218.
[9] Duncan, W. J. et al. 1984. The effect of environment on the strength of optical fiber. In: *Strength of Inorganic Glasses* (C. R. Kurkjian, ed.), pp. 309–328. Plenum Press, New York.
[10] Matthewson, M. J. 1994. Optical fiber mechanical testing techniques. *Proc. Soc. Photo-Opt. Instrum. Eng. Crit. Rev.* CR50:32–59.

[11] Kraus, J. et al. 2002. Bending strength and fractographic analysis of zinc tellurite glass modified fibres. *Proc. Soc. Photo-Opt. Instrum. Eng*. 4639:30–39.
[12] Merwin H. E. and E. S. Larsen. 1912. Mixtures of amorphous sulphur and selenium as immersion media for the determination of high refractive indices with the microscope. *Am. J. Sci*. 34:42–47.
[13] Dewald, J. F. et al. 1962. *J. Electrochem. Soc*. 109:243C.
[14] Kolomiets, B. T. and E. A. Lebedev. 1963. *Radiotecknika i Radioelectronika* 8:2037.
[15] Poulain, M. et al. 1975. Verres fluores au tetrafluorure de zirconium proprietes optiques d'un verre dope au Nd^{3+}. *Mat. Res. Bull*. 10(4):243–246.
[16] Harrington, J. A. 2004. *Infrared Fibers and Their Applications*. SPIE Press, Bellingham, WA.
[17] Proctor, B. A. et al. 1967. The strength of fused silica. *Proc. Roy. Soc*. A297:534–557.
[18] Weibull, W. 1951. A statistical distribution of wide applicability. *J. Appl. Mech*. 18.
[19] Matthewson, M. J. et al. 1986. Strength measurement of optical fibers by bending. *J. Am. Ceram. Soc*. 69:815.
[20] Krause, J. T. et al. 1979. Deviations from linearity in the dependence of elongation upon force for fibres of simple glass formers and of glass optical lightguides. *Phys. Chem. Glasses* 20(6):135–139.
[21] Glaesemann, G. S. et al. 1988. Effect of strain and surface composition on Young's modulus of optical fibers. *OFC'88 Tech. Digest* 48.
[22] Griffioen, W. 1992. Effect of nonlinear elasticity on measured fatigue data and lifetime estimations of optical fibers. *J. Am. Ceram. Soc*. 75(10):2692–2696.
[23] France, P. W. et al. 1980. Liquid nitrogen strengths of coated optical glass fibres. *J. Mat. Sci*. 15:825–830.
[24] Ernsberger, F. M. 1969. Tensile and compressive strength of pristine glasses by an oblate bubble technique. *Phys. Chem Glasses* 10(6):240–245.
[25] Lower, N. P. 2004. Failure studies of glass fibers, PhD thesis. University of Missouri, Rolla, MO.
[26] Kurkjian, C. R. et al. 2003. The intrinsic strength and fatigue of oxide glasses. *J. Non-Cryst. Solids* 316:114–124.
[27] Inniss, D. et al. 1993. Chemically corroded pristine silica fibers: Sharp or blunt flaws? *J. Am. Ceram. Soc*. 76:3173.
[28] Griffith, A. A. 1920. The phenomena of rupture and flow in solids. *Phil. Trans. Roy. Soc*. A221:163.
[29] Otto, W. H. 1955. Relationship of tensile strength of glass fibers to diameter. *J. Am. Ceram. Soc*. 38:122.
[30] Cameron, N. M. 1968. The effect of environment and temperature on the strength of E-glass fibres, Pt. 1. High vacuum and low temperature. *Glass Tech*. 9(1):14.
[31] Kurkjian, C. R. and U. C. Paek. 1983. Single-valued strength of "perfect" silica fibers. *Appl. Phys. Lett*. 42:251.
[32] Smith, W. A. and T. M. Michalske. 1990. Report for DOE contract no. DE-AC04-70DPOO789.
[33] Mazur, E. 2004. Personal communication.
[34] Lin, B. L. and M. J. Matthewson. 1996. "Diameter Dependence of the Strength of Optical Fibers." Unpublished work.
[35] Armstrong, J. L. et al. 2000. Humidity dependence of the fatigue of high-strength fused silica optical fibers. *J. Am. Ceram. Soc*. 83(12):3100–3108.
[36] Taylor, A. T. and M. J. Matthewson. 1998. Effect of pH on the strength and fatigue behavior of fused silica optical fiber. In: *Proc. 47th Int. Wire Cable Symp,* pp. 874–879. INCS, Eatontown, NJ.

[37] Glaesemann, G. S. 2006. Personal communication.
[38] Kurkjian, C. R. 1977. Tensile strengths of polymer coated fibers for use in optical communications. In: *Proc. XI Int. Cong. Glass,* p. 469.
[39] Breuls, A. 1993. A COST comparison of *n* values obtained with different techniques. In: *COST Proc. Turin*.
[40] Krause, J. T. 1979. Transitions in the static fatigue of fused silica fiber lightguides. In: *Proc. 5th ECOC, Postdeadline paper* 19.1-1–19.1-4.
[41] Wang, T. T. and H. M. Zupko. 1978. Long-term mechanical behavior of optical fibres coated with a u.v.-curable epoxy. *J. Mat. Sci*. 13:2241–2248.
[42] Kurkjian, C. R. and M. J. Matthewson. 1996. Strength degradation of lightguide fibres in room temperature water. *Elec. Lett*. 32(8).
[43] Matthewson, M. J. and H. H. Yuce. 1994. Kinetics of degradation during fatigue and aging of fused silica optical fiber. *Proc. Soc. Photo-Opt. Instrum. Eng*. 2290:204–210.
[44] Krukjian, C. R. et al. 1996. Room temperature strength degradation of optical fibers. *SPIE, 2611* 34–37.
[45] Rondinella, V. V. et al. 1994. Coating additives for improved mechanical reliability of optical fiber. *J. Am. Ceram. Soc*. 77(1):73–80.
[46] Schneider, H. W. 1988. Strength in fluoride glass fibers. In: *Halide Glasses V*. (M. Yamane and C. T. Moynihan, eds.), pp. 561–570. Trans Tech Publications, Inc., Uetikon-Zurich.
[47] Carter, S. F. 1990. Mechanical properties. In: *Fluoride Glass Optical Fibres* (P. W. France et al., eds.), pp. 219–236. Blackie and CRC Press, Florida.
[48] Colaizzi, J. and M. J. Matthewson. 1994. Mechanical durability of ZBLAN and Aluminum fluoride-based optical fiber. *J. Lightwave Technol*. 12(8):1317–1324.
[49] Devyatkh, G. G. et al. 1999. Recent developments in As-S glass fibers. *J. Non-Cryst. Solids* 256/257:318–322.
[50] Sanghera, J. 2005. Strength of arsenic sulfide fibers. Personal communication.
[51] Dianov, E. M. et al. 1990. Mechanical properties of chalcogenide glass optical fibers. *Proc. SPIE* 1228:92–100.
[52] Zhou, J. et al. 2004. High tensile strength photonic crystal fibers. *OFC'04 Tech. Digest* WI2.
[53] Mrotek, J. L. et al. 2001. Diffusion of moisture through optical fiber coatings. *J. Lightwave Technol*. 19(7):988–993.
[54] Bogatyrjov, V. A. et al. 1988. High strength hermetically sealed optical fiber. *JETP Lett*. 14:343.
[55] Orcel, G. et al. 1995. Hermetic and polymeric coatings for military and commercial applications. *Proc. Int. Wire Cable Symp*. 330–334.
[56] Kurkjian, C. R. and H. Leidecker. 2001. Strength of carbon-coated fibers. *Proc. Soc. Photo-Opt. Instrum. Eng*. 4215:134–143.
[57] Kurkjian, C. R. 2006. Distribution of stripping-induced flaws. *Proc. Soc. Photo-Opt. Instrum. Eng*. 4215:150–157.
[58] Rondinella, V. V. and M. J. Matthewson. 1993. Effect of chemical stripping on the strength and surface morphology of fused silica optical fiber. *Proc. Soc. Photo-Opt. Instrum. Eng*. 2074:52–58.
[59] Matthewson, M. J. et al. 1997. Acid stripping of fused silica optical fibers without strength degradation. *J. Lightwave Technol*. 15(3):490–497.
[60] Park, H. S. et al. 1999. A novel method of removing optical fiber coating with hot air stream. *OFC/IOOC99 Tech. Digest* 2:371–373.
[61] Castilone, R. J. et al. 2002. Relationship between mirror dimensions and failure stress for optical fibers. *Proc. Soc. Photo-Opt. Instrum. Eng*. 4639:11–20.
[62] Krause, J. T. et al. 1981. Strength of fusion splices for fibre lightguides. *Elec. Lett*. 17:232.

[63] Krause, J. T. 1986. Ultrahigh strength fibre fusion splices by modified H_2/O_2 flame fusion. *Elec. Lett*. 22:1075–1076.
[64] Simpkins, P. G. and C. R. Kurkjian. 1995. Aluminum-coated silica fibres: Strength and solderability. *Elec. Lett*. 31(9):747–748.
[65] Bogatyrjov, V. A. et al. 1992. Heat resistant optical fibers hermetically sealed in aluminum. *Tech. Phys. Lett*. 8(698):699.
[66] Proctor, B. A. 1962. The effects of hydrofluoric acid etching on the strength of glass. *Phys. Chem Glasses* 3(1):7–27.
[67] Vitman, F. F. et al. 1996. Influence of temperature on the strength of etched fused quartz glass in its high strength state. *Sov. Phys. Sol. State* 8(5):1195.
[68] Miyama, Y. et al. 1983. Submarine optical-fiber cable containing high-strength splices. *J. Lightwave Tech*. 1(1):184–189.
[69] Kurkjian, C. R. et al. 2004. Effects of heat treatment and HF etching on the strength of silica lightguides. *Proc. Soc. Photo-Opt. Instrum. Eng*. 5465:223–229.
[70] Kurkjian, C. R. et al. 2006. Recovery of strength caused by HF etching. Unpublished work.
[71] Castilone, R. J. et al. 2000. Extrinsic strength measurements and associated mechanical reliability modeling of optical fiber. *Proc. 16th NFOEC*.
[72] Technical report on the power-law theory of optical fibre reliability. IEC SC86A/WG1 NO-17A, IEC (March, 1997).
[73] Mitsunaga, Y. et al. 1982. Failure prediction for long length optical fiber based on proof testing. *J. Appl. Phys*. 53(7):4847–4853.